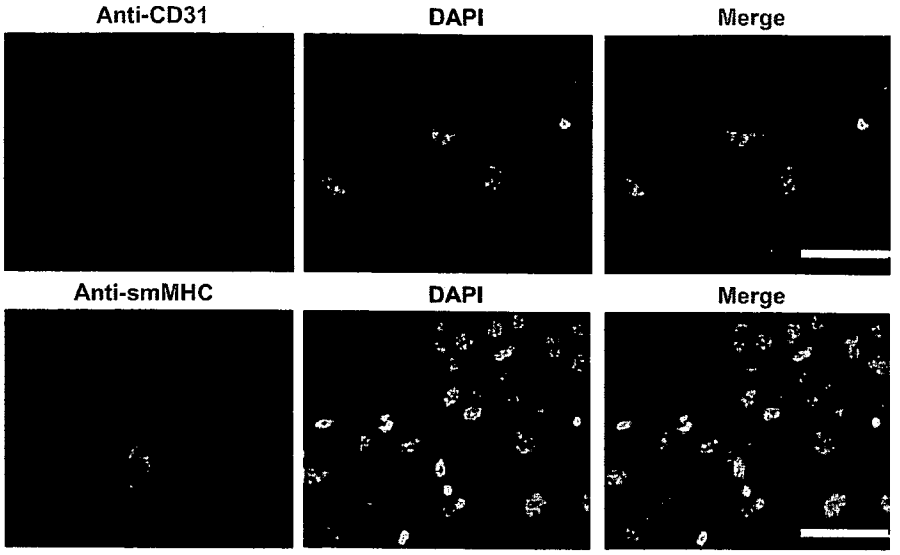

Fig. 4. MDPCs maintain a capacity of differentiation into cardiovascular lineages after treatment with OPN. Immunostaining was performed using an anti-CD31 antibody or an anti-smMHC antibody. MDPCs treated with OPN were differentiated into CD31 positive endothelial (red) or smMHC positive smooth muscle (red) cells by VEGF or PDGF, respectively. Nuclei were stained by DAPI (blue). Bar indicates 50 μm.

effects on HSC and MDPC proliferation is unclear. HSCs have been shown to express several integrins and various isoforms of CD44 [32]. Except for the expression of CD44 and β1 integrin on MDPCs [6], it remains to be determined whether isoforms of CD44 and other integrins are expressed on MDPCs. Since the different effects that OPN elicits can be attributed to its multiple receptors, binding sites, and various forms [33], the expression pattern of integrins and CD44 isoforms in MDPCs may differ from that in HSCs.

In conclusion, we identified OPN as a secreted molecule in MDPCs by using SAGE and SST. Recombinant OPN had a proliferative effect on MDPCs with or without various growth factors, and PI3K/Akt signaling was involved in the effect. Furthermore, MDPCs treated with OPN had an enhanced proliferative potential and maintained their potency to differentiate into vascular lineages. Thus, OPN may be one of the candidate autocrine/paracrine molecules that could be applied in a therapeutic intervention using MDPCs to treat patients with vascular diseases.

Acknowledgments

We are grateful to Ms. A. Kosugi, Ms. M. Nishikawa, and Mr. M. Kuramoto for their skillful technical assistance. This work was supported by Grants-in-Aid from the Ministry of Education, Culture, Sports, Science and Technology of Japan, and by Grants-in-Aid from the Ministry of Health, Labor, and Welfare of Japan, Japan Association for the Advancement of Medical Equipment, Takeda Science Foundation, Novartis Research Award on Molecular and Cellular Cardiology, Kanae Foundation for Life & Socio-Medical Science, Suzuken Memorial Foundation, and Mochida Memorial Foundation.

References

[1] Z. Qu-Petersen, B. Deasy, R. Jankowski, M. Ikezawa, J. Cummins, R. Pruchnic, J. Mytinger, B. Cao, C. Gates, A. Wernig, J. Huard, Identification of a novel population of muscle stem cells in mice: potential for muscle regeneration, J. Cell Biol. 157 (2002) 851–864.

[2] H. Oshima, T.R. Payne, K.L. Urish, T. Sakai, Y. Ling, B. Gharaibeh, K. Tobita, B.B. Keller, J.H. Cummins, J. Huard, Differential myocardial infarct repair with muscle stem cells compared to myoblasts, Mol. Ther. 12 (2005) 1130–1141.

[3] T.R. Payne, H. Oshima, T. Sakai, Y. Ling, B. Gharaibeh, J. Cummins, J. Huard, Regeneration of dystrophin-expressing myocytes in the mdx heart by skeletal muscle stem cells, Gene Ther. 12 (2005) 1264–1274.

[4] T. Tamaki, A. Akatsuka, K. Ando, Y. Nakamura, H. Matsuzawa, T. Hotta, R.R. Roy, V.R. Edgerton, Identification of myogenic-endothelial progenitor cells in the interstitial spaces of skeletal muscle, J. Cell Biol. 157 (2002) 571–577.

[5] R. Sarig, Z. Baruchi, O. Fuchs, U. Nudel, D. Yaffe, Regeneration and transdifferentiation potential of muscle-derived stem cells propagated as myospheres, Stem Cells 24 (2006) 1769–1778.

[6] T. Nomura, E. Ashihara, K. Tateishi, S. Asada, T. Ueyama, T. Takahashi, H. Matsubara, H. Oh, Skeletal myosphere-derived progenitor cell transplantation promotes neovascularization in δ-sarcoglycan knockdown cardiomyopathy, Biochem. Biophys. Res. Commun. 352 (2007) 668–674.

[7] P. Taupin, J. Ray, W.H. Fischer, S.T. Suhr, K. Hakansson, A. Grubb, F.H. Gage, FGF-2-responsive neural stem cell proliferation requires CCg, a novel autocrine/paracrine cofactor, Neuron 28 (2000) 385–397.

[8] Y. Arsenijevic, S. Weiss, B. Schneider, P. Aebischer, Insulin-like growth factor-I is necessary for neural stem cell proliferation and demonstrates distinct actions of epidermal growth factor and fibroblast growth factor-2, J. Neurosci. 21 (2001) 7194–7202.

[9] H. Toda, M. Tsuji, I. Nakano, K. Kobuke, T. Hayashi, H. Kasahara, J. Takahashi, A. Mizoguchi, T. Houtani, T. Sugimoto, N. Hashimoto, T.D. Palmer, T. Honjo, K. Tashiro, Stem cell-derived neural

stem/progenitor cell supporting factor is an autocrine/paracrine survival factor for adult neural stem/progenitor cells, J. Biol. Chem. 278 (2003) 35491–35500.
[10] T. Nakamura, P. Ruiz-Lozano, V. Lindner, D. Yabe, M. Taniwaki, Y. Furukawa, K. Kobuke, K. Tashiro, Z. Lu, N.L. Andon, R. Schaub, A. Matsumori, S. Sasayama, K.R. Chien, T. Honjo, DANCE, a novel secreted RGD protein expressed in developing, atherosclerotic, and balloon-injured arteries, J. Biol. Chem. 274 (1999) 22476–22483.
[11] T. Kojima, T. Kitamura, A signal sequence trap based on a constitutively active cytokine receptor, Nat. Biotechnol. 17 (1999) 487–490.
[12] V.E. Velculescu, B. Vogelstein, K.W. Kinzler, Analysing uncharted transcriptomes with SAGE, Trends Genet. 16 (2000) 423–425.
[13] S.B. Rodan, G. Wesolowski, K. Yoon, G.A. Rodan, Opposing effects of fibroblast growth factor and pertussis toxin on alkaline phosphatase, osteopontin, osteocalcin, and type I collagen mRNA levels in ROS 17/2.8 cells, J. Biol. Chem. 264 (1989) 19934–19941.
[14] H. Rangaswami, A. Bulbule, G.C. Kundu, Osteopontin: role in cell signaling and cancer progression, Trends Cell Biol. 16 (2006) 79–87.
[15] K. Tateishi, E. Ashihara, S. Honsho, N. Takehara, T. Nomura, T. Takahashi, T. Ueyama, M. Yamagishi, H. Yaku, H. Matsubara, H. Oh, Human cardiac stem cells exhibit mesenchymal features and are maintained through Akt/GSK-3β signaling, Biochem. Biophys. Res. Commun. 352 (2007) 635–641.
[16] D.N. Haylock, S.K. Nilsson, Osteopontin: a bridge between bone and blood, Br. J. Haematol. 134 (2006) 467–474.
[17] S. Temple, A. Alvarez-Buylla, Stem cells in the adult mammalian central nervous system, Curr. Opin. Neurobiol. 9 (1999) 135–141.
[18] A. Gritti, E.A. Parati, L. Cova, P. Frolichsthal, R. Galli, E. Wanke, L. Faravelli, D.J. Morassutti, F. Roisen, D.D. Nickel, A.L. Vescovi, Multipotential stem cells from the adult mouse brain proliferate and self-renew in response to basic fibroblast growth factor, J. Neurosci. 16 (1996) 1091–1100.
[19] B.A. Reynolds, S. Weiss, Clonal and population analyses demonstrate that an EGF-responsive mammalian embryonic CNS precursor is a stem cell, Dev. Biol. 175 (1996) 1–13.
[20] E. Messina, L. De Angelis, G. Frati, S. Morrone, S. Chimenti, F. Fiordaliso, M. Salio, M. Battaglia, M.V. Latronico, M. Coletta, E. Vivarelli, L. Frati, G. Cossu, A. Giacomello, Isolation and expansion of adult cardiac stem cells from human and murine heart, Circ. Res. 95 (2004) 911–921.
[21] Y.H. Lin, H.F. Yang-Yen, The osteopontin-CD44 survival signal involves activation of the phosphatidylinositol 3-kinase/Akt signaling pathway, J. Biol. Chem. 276 (2001) 46024–46030.
[22] R. Das, G.H. Mahabeleshwar, G.C. Kundu, Osteopontin stimulates cell motility and nuclear factor κB-mediated secretion of urokinase type plasminogen activator through phosphatidylinositol 3-kinase/Akt signaling pathways in breast cancer cells, J. Biol. Chem. 278 (2003) 28593–28606.
[23] Y.U. Katagiri, J. Sleeman, H. Fujii, P. Herrlich, H. Hotta, K. Tanaka, S. Chikuma, H. Yagita, K. Okumura, M. Murakami, I. Saiki, A.F. Chambers, T. Uede, CD44 variants but not CD44s cooperate with β1-containing integrins to permit cells to bind to osteopontin independently of arginine-glycine-aspartic acid, thereby stimulating cell motility and chemotaxis, Cancer Res. 59 (1999) 219–226.
[24] H.C. Crawford, L.M. Matrisian, L. Liaw, Distinct roles of osteopontin in host defense activity and tumor survival during squamous cell carcinoma progression in vivo, Cancer Res. 58 (1998) 5206–5215.
[25] Y. Wu, D.T. Denhardt, S.R. Rittling, Osteopontin is required for full expression of the transformed phenotype by the ras oncogene, Br. J. Cancer 83 (2000) 156–163.
[26] S.R. Rittling, A.F. Chambers, Role of osteopontin in tumour progression, Br. J. Cancer 90 (2004) 1877–1881.
[27] D. Denhardt, Osteopontin expression correlates with melanoma invasion, J. Invest. Dermatol. 124 (2005) xvi–xviii.
[28] A. Hirata, S. Masuda, T. Tamura, K. Kai, K. Ojima, A. Fukase, K. Motoyoshi, K. Kamakura, Y. Miyagoe-Suzuki, S. Takeda, Expression profiling of cytokines and related genes in regenerating skeletal muscle after cardiotoxin injection: a role for osteopontin, Am. J. Pathol. 163 (2003) 203–215.
[29] Y. Asou, S.R. Rittling, H. Yoshitake, K. Tsuji, K. Shinomiya, A. Nifuji, D.T. Denhardt, M. Noda, Osteopontin facilitates angiogenesis, accumulation of osteoclasts, and resorption in ectopic bone, Endocrinology 142 (2001) 1325–1332.
[30] S.K. Nilsson, H.M. Johnston, G.A. Whitty, B. Williams, R.J. Webb, D.T. Denhardt, I. Bertoncello, L.J. Bendall, P.J. Simmons, D.N. Haylock, Osteopontin, a key component of the hematopoietic stem cell niche and regulator of primitive hematopoietic progenitor cells, Blood 106 (2005) 1232–1239.
[31] S. Stier, Y. Ko, R. Forkert, C. Lutz, T. Neuhaus, E. Grunewald, T. Cheng, D. Dombkowski, L.M. Calvi, S.R. Rittling, D.T. Scadden, Osteopontin is a hematopoietic stem cell niche component that negatively regulates stem cell pool size, J. Exp. Med. 201 (2005) 1781–1791.
[32] P.J. Simmons, J.P. Levesque, A.C. Zannettino, Adhesion molecules in haemopoiesis, Baillieres Clin. Haematol. 10 (1997) 485–505.
[33] D.T. Denhardt, X. Guo, Osteopontin: a protein with diverse functions, FASEB J. 7 (1993) 1475–1482.

Circulation
JOURNAL OF THE AMERICAN HEART ASSOCIATION

American Heart Association®
Learn and Live℠

Central Role of Calcium-Dependent Tyrosine Kinase PYK2 in Endothelial Nitric Oxide Synthase Mediated Angiogenic Response and Vascular Function

Akihiro Matsui, Mitsuhiko Okigaki, Katsuya Amano, Yasushi Adachi, Denan Jin, Shinji Takai, Tomoya Yamashita, Seinosuke Kawashima, Tatsuya Kurihara, Mizuo Miyazaki, Kento Tateishi, Shinsaku Matsunaga, Asako Katsume, Shoken Honshou, Tomosaburo Takahashi, Satoaki Matoba, Tetsuro Kusaba, Tetsuya Tatsumi and Hiroaki Matsubara

Circulation 2007;116;1041-1051; originally published online Aug 13, 2007;
DOI: 10.1161/CIRCULATIONAHA.106.645416
Circulation is published by the American Heart Association. 7272 Greenville Avenue, Dallas, TX 72514
 Print ISSN: 0009-7322. Online ISSN: 1524-4539

Central Role of Calcium-Dependent Tyrosine Kinase PYK2 in Endothelial Nitric Oxide Synthase–Mediated Angiogenic Response and Vascular Function

Akihiro Matsui, MD; Mitsuhiko Okigaki, MD, PhD; Katsuya Amano, MD, PhD; Yasushi Adachi, MD, PhD; Denan Jin, MD, PhD; Shinji Takai, PhD; Tomoya Yamashita, MD, PhD; Seinosuke Kawashima, MD, PhD; Tatsuya Kurihara, PhD; Mizuo Miyazaki, MD, PhD; Kento Tateishi, MD, PhD; Shinsaku Matsunaga, MD; Asako Katsume, MD; Shoken Honshou, MD; Tomosaburo Takahashi, MD, PhD; Satoaki Matoba, MD, PhD; Tetsuro Kusaba, MD; Tetsuya Tatsumi, MD, PhD; Hiroaki Matsubara, MD, PhD

Background—The involvement of Ca^{2+}-dependent tyrosine kinase PYK2 in the Akt/endothelial NO synthase pathway remains to be determined.

Methods and Results—Blood flow recovery and neovessel formation after hind-limb ischemia were impaired in $PYK2^{-/-}$ mice with reduced mobilization of endothelial progenitors. Vascular endothelial growth factor (VEGF)–mediated cytoplasmic Ca^{2+} mobilization and Ca^{2+}-independent Akt activation were markedly decreased in the PYK2-deficient aortic endothelial cells, whereas the Ca^{2+}-independent AMP-activated protein kinase/protein kinase-A pathway that phosphorylates endothelial NO synthase was not impaired. Acetylcholine-mediated aortic vasorelaxation and cGMP production were significantly decreased. Vascular endothelial growth factor–dependent migration, tube formation, and actin cytoskeletal reorganization associated with Rac1 activation were inhibited in PYK2-deficient endothelial cells. PI3-kinase is associated with vascular endothelial growth factor–induced PYK2/Src complex, and inhibition of Src blocked Akt activation. The vascular endothelial growth factor–mediated Src association with PLCγ1 and phosphorylation of ^{783}Tyr-PLCγ1 also were abolished by PYK2 deficiency.

Conclusion—These findings demonstrate that PYK2 is closely involved in receptor- or ischemia-activated signaling events via Src/PLCγ1 and Src/PI3-kinase/Akt pathways, leading to endothelial NO synthase phosphorylation, and thus modulates endothelial NO synthase–mediated vasoactive function and angiogenic response. (***Circulation.*** **2007;116: 1041-1051.)**

Key Words: angiogenesis ■ endothelium ■ nitric oxide synthase ■ signal transduction ■ vasodilation

Nitric oxide (NO) has multiple functions in NO-mediated vascular action and angiogenic response. This was confirmed by endothelial NO synthase $(eNOS)^{-/-}$ mice exhibiting hypertension[1] or impaired vascular endothelial growth factor (VEGF) –induced angiogenesis.[2] VEGF phosphorylates eNOS, which is directly activated on the phosphorylation of ^{1177}serine in human (^{1176}serine in mouse) by Akt,[3,4] whereas the upstream molecules that activate Akt-eNOS system have not been fully clarified.

Clinical Perspective p 1051

Tyrosine kinases activate the PI3-kinase/Akt or Ca^{2+} signaling pathways, suggesting that tyrosine kinase is upstream of eNOS. Indeed, Src and VEGF receptor-2 activate eNOS through activation of the PI3-kinase/Akt pathway.[5] PYK2 (proline-rich tyrosine kinase), also known as RAFTK, CAK, and CADTK,[6,7] is the cytoplasmic tyrosine kinase and exhibits 45% amino acid sequence

Received August 9, 2005; accepted June 12, 2007.

From the Department of Cardiovascular Medicine, Kyoto Prefectural University School of Medicine, Kyoto (A.M., M.O., K.T., S.M., A.K., S.H., T. Takahashi, S.M., T. Kusaba, T. Tatsumi, H.M.); Departments of Internal Medicine II (K.A.) and Pathology I (Y.A.), Kansai Medical University, Osaka; Department of Pharmacology, Osaka Medical College, Takatsuki (D.J., S.T., M.M.); Division of Cardiovascular and Respiratory Medicine, Kobe University School of Medicine, Kobe (T.Y., S.K.); and Daiichi Asubio Pharma Co Ltd Biomedical Research Laboratories, Osaka (T. Kurihara), Japan.

The online Data Supplement, consisting of an expanded Methods section and a figure, can be found with this article at http://circ.ahajournals.org/cgi/content/full/CIRCULATIONAHA.106.645416/DC1.

Correspondence to Mitsuhiko Okigaki, MD, Department of Cardiovascular Medicine, Kyoto Prefectural University of Medicine, Kamigyo-ku, Kyoto, 602–8566, Japan. E-mail okigakim@koto.kpu-m.ac.jp

Circulation **is available at http://circ.ahajournals.org**

DOI: 10.1161/CIRCULATIONAHA.106.645416

identity to focal adhesion kinase. Tyrosine phosphorylation of PYK2 and focal adhesion kinase was triggered by integrin-mediated adhesion.[8] PYK2 was stimulated by a broad range of physiological stimuli such as stimuli for G-protein–coupled receptors that elevate intracellular Ca^{2+},[6,7] phorbol ester, inflammatory cytokines, and stress signals, including ischemia.[9] PYK2 acts in concert with Src, which links Gi- or Gq-coupled receptors, leading to the MAP kinase pathway.[10] Furthermore, PYK2 binds to proteins that interact with the cytoskeleton, suggesting a role in the regulation of cellular morphology. The phenotype of PYK2-deficient mice was recently described as having macrophages that exhibit impaired migration as a result of cytoskeleton abnormality induced by diminished Ca^{2+} mobilization and reduced activation of PI3-kinase.[11] In this study, we newly generated $PYK2^{-/-}$ mice and investigated the molecular mechanism for the effects of PYK2 on NO-mediated vascular function and angiogenic response.

Methods

Statistical Analysis

Results are expressed as mean±SEM. All data were transformed by the natural logarithm before ANOVA corresponding to each experiment. Repeated-measures ANOVA was used to analyze the time course experiment. The Scheffé test was used as the multiple comparison test. For comparisons between 2 groups, a 2-sample *t* test was performed. A value of $P< 0.05$ (2 tailed) was considered statistically significant.

Materials, construction of targeting vector, generation of $PYK2^{-/-}$ mice (Figure I of the online Data Supplement), Western blotting, immunohistochemistry, transfection of DNA plasmid, measurement of GTP-Rho and GTP-Rac, migration, tubular formation, in vivo angiogenesis, preparation of endothelial progenitor cell (EPC) –like cells, hind-limb ischemia, laser Doppler perfusion image, cGMP assay, measurement of NO metabolites and NO levels, acetylcholine (Ach)- and nitroprusside-mediated vasodilatation, measurement of cytoplasmic Ca^{2+} concentration, fluorescence-activated cell sorting, and isolation of endothelial cells (ECs) from aorta and primary culture are described in the Methods section of the online Data Supplement. C57B1/6 strain mice (SHIMIZU Laboratory Supplies, Kyoto, Japan) were used. The animal experiments were approved by our institutional review board.

The authors had full access to and take full responsibility for the integrity of the data. All authors have read and agree to the manuscript as written.

Results

Impaired eNOS/Akt Activation and Ca^{2+} Mobilization by PYK2 Deficiency

eNOS was reported to be activated by VEGF, Ach, or ischemic stress.[12] Incubation of the aorta with VEGF (100 ng/mL) phosphorylates PYK2 time dependently with a peak level around 5 minutes (Figure 1A). Ach (1 μmol/L) also caused PYK2 phosphorylation with a similar peak level, the extent of which was comparable to that in VEGF stimulation (Figure 1A). Ischemic stress time dependently increased the phosphorylation of PYK2 in the hind-limb muscle (Figure 1B). Such PYK2 phosphorylation was observed in the primary cultured aortic von Willebrand factor–positive ECs after stimulation with VEGF (100 ng/mL) and Ach (1 μmol/L) and exposure to 1% hypoxia (Figure 1C). To clarify the cell types expressing PYK2, an immunohistochemical analysis was performed. Figure 1D showed that PYK2 was present mainly in the endothelial ($CD31^+$ ECs) and medial layers (vascular smooth muscle cells) in the aorta and in the $CD31^+$ vessels in the skeletal muscle, in which a few cells in the interstitial region ($CD31^-$) also expressed PYK2.

We next examined whether the stimuli that induce PYK2 activation led to the phosphorylation of eNOS. Hind-limb ischemia causes eNOS phosphorylation in the skeletal muscle in wild-type (+/+) mice, whereas eNOS activation in the $PYK2^{-/-}$ mice was markedly inhibited (Figure 2A). Exposure of the aorta to VEGF or Ach also induced eNOS phosphorylation, whereas their activated levels were significantly diminished in the $PYK2^{-/-}$ mice (Figure 2B). Induction of eNOS phosphorylation by VEGF or Ach or exposure to 1% hypoxia also was observed (2.3- to 2.5-fold, respectively; $P<0.005$) in the wild-type aortic ECs but strongly inhibited in the PYK2-deficient ECs (Figure 2C).

The ischemia-induced Akt phosphorylation in the skeletal muscle was significantly lower in the $PYK2^{-/-}$ mice (46±3% at 2 hours, 34±3% decrease 1 day after ischemia; $P<0.01$) than the wild-type mice (Figure 2A), whereas the tyrosine phosphorylation level in VEGF receptor-2 (Flk-1) did not significantly differ between the wild-type and PYK2-deficient muscle (n=6 each; data not shown).

Akt phosphorylation in the aorta (Figure 2B) and ECs (Figure 2C) from the wild-type mice was significantly increased by VEGF stimulation (1.7±0.3-fold, $P<0.05$; and 3.0±0.7-fold, $P<0.005$, respectively), whereas Akt activation in the PYK2-deficient aorta and ECs was markedly attenuated (43±3% and 42±6% inhibition, respectively; $P<0.05$). Significant inhibition of Akt phosphorylation in ECs by PYK2 deficiency also was observed after exposure to 1% hypoxia (72±5% inhibition; $P<0.01$; Figure 2C).

We examined the involvement of AMP-activated protein kinase (AMPK)[13] and cAMP-dependent protein kinase-A (PKA),[14] known as the Ca^{2+}-independent kinase for phosphorylation of ^{1176}Ser-eNOS. The phosphorylation levels of AMPK and PKA after hind-limb ischemia did not differ significantly between $PYK2^{-/-}$ and wild-type mice (Figure 2A). Furthermore, the phosphorylation of AMPK and PKA in PYK2-deficient ECs exposed to 1% hypoxia for 18 hours also was similar to the wild-type ECs (data not shown). Akt, AMPK, and PKA showed peak phosphorylation on day 1 and at 2 hours, respectively; PKA and AMPK then reversed to baseline levels on day 7, whereas moderate activation of Akt was observed on day 7 (220±30% increase compared with basal level; Figure 2A). Neither AMPK nor PKA was activated 5 minutes after VEGF (100 ng/mL) treatment in both the wild-type and PYK2-deficient cells (data not shown), whereas dibutylic cAMP (1 mmol/L) and 5-aminoimidazole-4-carboxamide-1-β-D-riboside AICAR (1 mmol/L) apparently phosphorylated PKA and AMPK in the wild-type ECs (positive controls; data not shown). These findings suggest that Akt, rather than Ca^{2+}-independent AMPK or PKA, is involved in VEGF-mediated eNOS phosphorylation.

To prove that the reduced phosphorylation of eNOS is due directly to the loss of PYK2, we transfected GFP-tagged PYK2 plasmid to the PYK2-deficient ECs and studied by

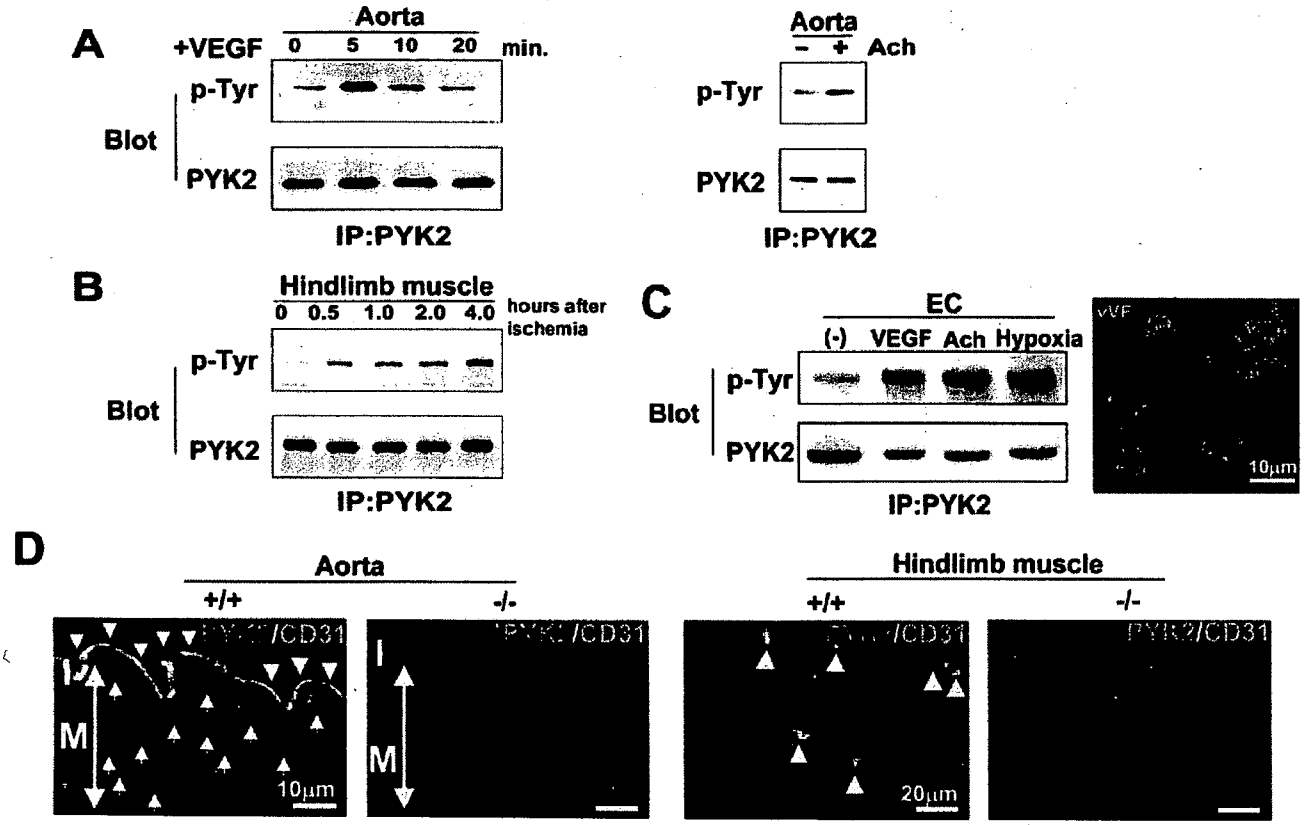

Figure 1. Activation of PYK2 by VEGF, Ach, and hind-limb ischemia. A, Aortic tissue removed from wild-type mice was incubated with the medium including VEGF (100 ng/mL) or Ach (1 μmol/L) for 5 minutes. B, Time-dependent PYK2 phosphorylation in hind-limb muscles was examined after ligation of femoral artery. C, Left, Aortic ECs were stimulated with VEGF (100 ng/mL) or Ach (1 μmol/L) for 5 minutes or exposure with 1% hypoxia for 18 hours. Tissue or cell lysates were subjected to immunoprecipitation with an anti-PYK2 antibody, followed by immunoblotting with anti-phosphotyrosine or anti-PYK2 antibodies. Data are mean±SE (n=5 each); representative results are shown. Right, Cells were immunostained with anti–von Willebrand factor antibody to identify the ECs. D, Distribution of PYK2 in the aorta and limb muscle. Aorta and limb muscle were frozen-sectioned, fixed with acetone, and subjected to double immunostaining with antibodies against PYK2 (green) and CD31 (red). The merged cells (yellow) are indicated by arrowheads; PYK2-positive smooth muscle in the aorta, by arrows. I indicates intima; M, media.

immunostaining with anti–phospho-^{1176}Ser-eNOS antibody whether VEGF-mediated phosphorylation of eNOS can be restored (Figure 2D). eNOS phosphorylation was observed in VEGF-exposed cells in which GFP-tagged PYK2 plasmid was transfected, whereas phospho-eNOS–positive cells were barely detected in the control GFP-transfected cells.

We next studied whether intracellular Ca^{2+} mobilization was influenced by PYK2 deficiency. Figure 3A shows that VEGF-mediated elevation of cytoplasmic Ca^{2+} levels was markedly inhibited in the PYK2-deficient ECs (Ca^{2+} concentrations in PYK2$^{-/-}$, 95±24 nmol/L versus wild type, 432±69 nmol/L; $P<0.001$), whereas Ca^{2+} mobilization with ATP that directly opens the Ca^{2+} channel on the plasma membrane[15] was comparable to the wild type (Figure 3A), suggesting that the pathway for the receptor-independent Ca^{2+} mobilization is not impaired. To study the effect of PYK2 deficiency on the other Ca^{2+} signaling pathway not involving NO formation, we studied the activation of the Ca^{2+}-dependent transcription factor nuclear factor of activated T cells 2 (NFATc2), which was shown to be crucial for VEGF-mediated angiogenesis.[16] The results showed that 68±8% of the wild-type cells showed nuclear translocation of NFATc2 from cytoplasm 30 minutes after VEGF stimulation, whereas in the PYK2-deficient cells, the translocation was markedly reduced (22±6%; $P<0.01$), indicating that PYK2 deficiency inhibits Ca^{2+} signaling pathway not involving NO formation (Figure 3B). To prove that the functional effects are due directly to the loss of PYK2, we transfected the GFP-tagged PYK2 plasmid to the PYK2-deficient cells and observed VEGF-mediated nuclear translocation of NFATc2. In the PYK2-deficient cells transfected with GFP-tagged PYK2 plasmid, the number of NFATc2-translocated cells increased significantly (from 22±6% to 48±9%; $P<0.05$; Figure 3B), whereas in the control GFP-transfected cells, the translocated cells did not increase significantly (data not shown). Pretreatment with a chelator of intracellular Ca^{2+} store, AM-BAPTA (5 μmol/L), in the Ca^{2+}-free medium for 45 minutes did not affect VEGF-induced Akt activation in ECs (Figure 3C), indicating that Akt activation is Ca^{2+} independent in our system.

Reduced Response by PYK2 Deficiency in NO Production and Ach-Mediated Vasodilatation

The intracellular NO level was measured with 4-amino-5-methyl-amino-2′,7′-difluorofluorescein diacetate (DAF-FM DA). NO was visualized as green under laser

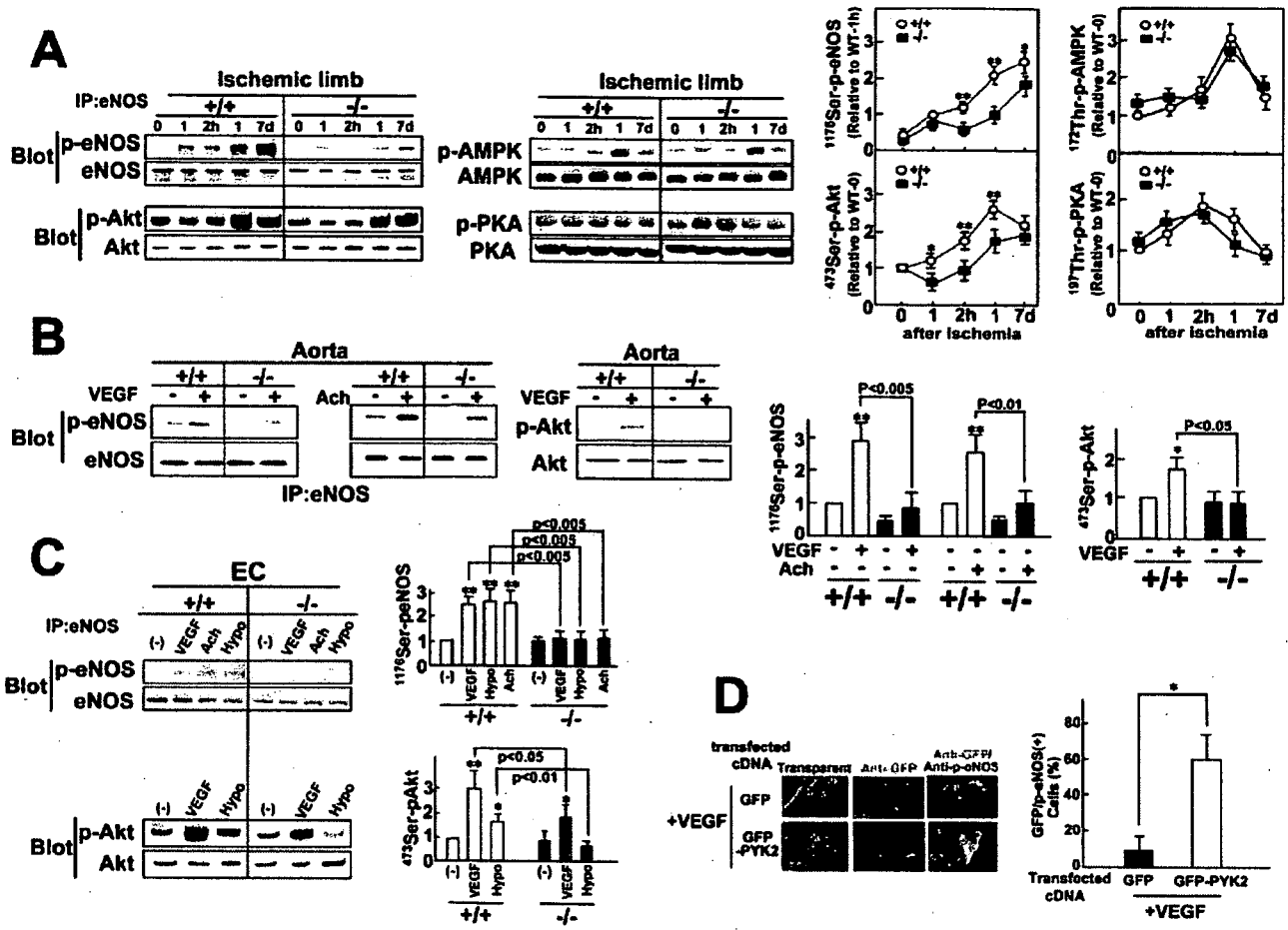

Figure 2. Impaired eNOS/Akt activation in PYK2-deficient mice. A, Skeletal muscle (n=10) was excised at the indicated time after ischemia. B, Aortic tissue (n=6 for each stimuli) was stimulated with VEGF (100 ng/mL) or Ach (1 μmol/L) for 5 minutes. C, Aortic ECs (n=6 for each stimuli) were stimulated with VEGF (100 ng/mL) or Ach (1 μmol/L) for 5 minutes or 1% hypoxia for 18 hours (n=6 each). Cell lysates were subjected to immunoprecipitation with anti-eNOS antibody, followed by immunoblot with antibodies against ^{1176}Ser-phosphorylated eNOS or eNOS. In addition, lysates were immunoblotted with antibodies against ^{473}Ser-phosphorylated Akt or Akt. Relative phosphorylation levels of eNOS and Akt are shown. Open circles and closed squares indicate the wild-type and PYK2$^{-/-}$ mice, respectively. A, *P<0.05, **P<0.01 vs the same time points of the PYK2$^{-/-}$ mice. B, C, *P<0.05, **P<0.005 vs the nonstimulated control. D, Aortic ECs were transfected with GFP- or GFP-PYK2-cDNA-plasmid. Forty-eight hours after transfection, cells were stimulated with VEGF (100 ng/mL), fixed with 4% paraformaldehyde, permeabilized with 0.02% Triton/PBS, and immunostained with antibodies against GFP- (red) or ^{1176}Ser-phosphorylated eNOS (green). Ratio of the GFP/p-eNOS double-positive cells (%) (yellow) to the total GFP-positive cells (red) was evaluated. *P<0.005; n=4.

microscopy (Figure 4A). In the wild-type ECs, VEGF increased NO levels by 3.2-fold (P<0.005 versus untreated cells); whereas this increase was severely impaired in the PYK2-deficient ECs. NO metabolites in the 24-hour urine sample were significantly lower in the PYK2$^{-/-}$ mice than the wild-type mice (4084±820 versus 9326±1163 nmol; P<0.005; Figure 4B). Oral administration of N^G-nitro-L-arginine methyl ester (L-NAME; 3 mmol/L in drinking water) to the wild-type mice reduced the NO metabolite production to a level comparable to the PYK2$^{-/-}$ mice (Figure 4B).

Ach-mediated vasodilatation is induced by the eNOS-NO system. We next examined whether Ach-mediated relaxation of the aorta is influenced by PYK2 deficiency. The dose-dependent relaxation of the isolated aorta constricted by norepinephrine was evaluated (Figure 4C). Ach (10 μmol/L) -mediated relaxation response was much weaker in the PYK2-deficient aorta than in the wild-type aorta (32±8% versus 59±5% relaxation; P<0.01), whereas norepinephrine (300 nmol/L) -mediated vasoconstriction in the PYK2-deficient aorta did not significantly differ from the wild-type aorta (190±30% versus 165±6% relative to 50 mmol/L KCl–mediated constriction; n=5). This result suggests that Ca^{2+} signaling transmitted mainly through voltage-dependent Ca^{2+} channel leading to the constriction of vascular smooth muscle cells is not impaired in the PYK2-deficient aorta.

To evaluate the NO dependency on Ach-mediated vasorelaxation, the effect of L-NAME was studied. Addition of L-NAME (10 μmol/L) markedly suppressed the Ach-mediated maximum relaxation of the wild-type aorta (from 59±5% to 17±2%; P<0.001; n=4), whereas in the PYK2-deficient aorta, the reduced relaxation response was suppressed further to a level comparable to L-NAME–treated

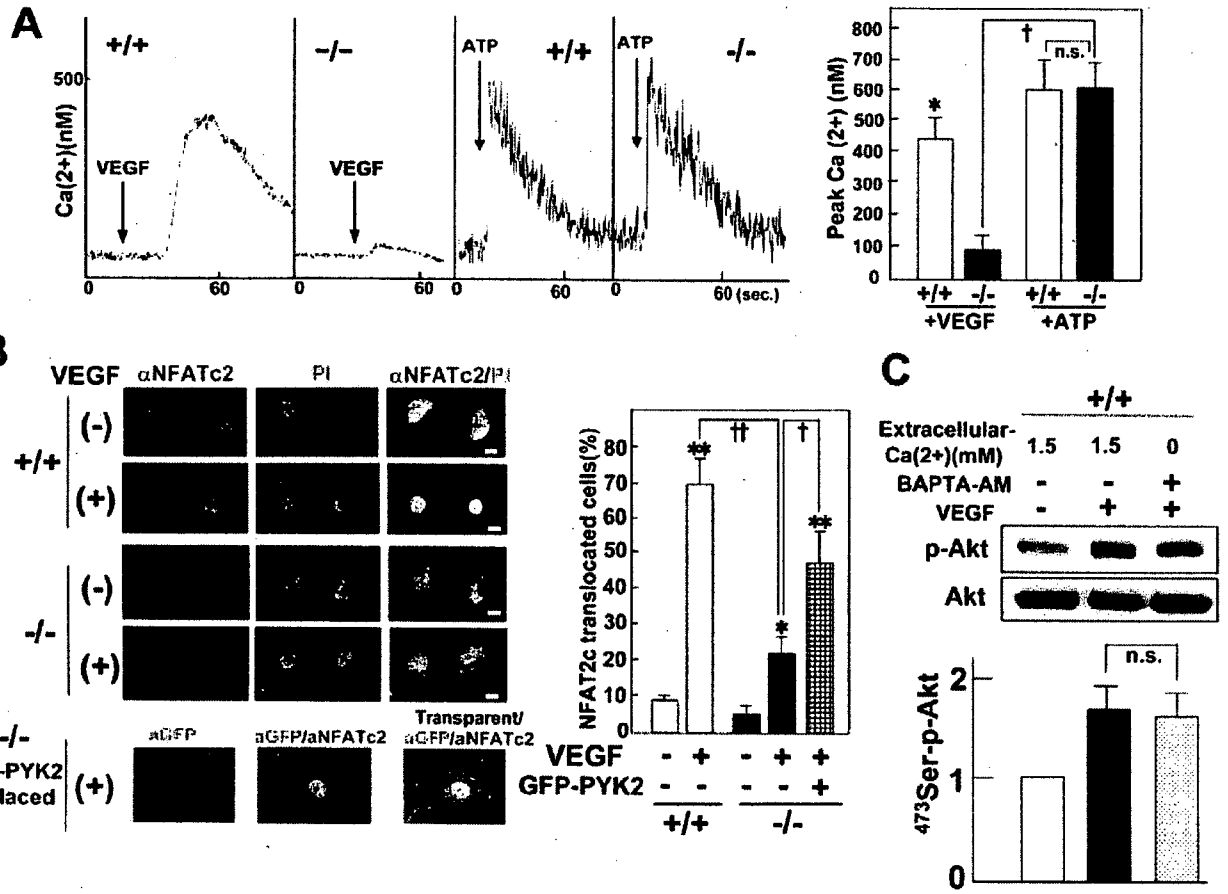

Figure 3. Impaired Ca^{2+} mobilization in PYK2-deficient mice. A, VEGF (100 ng/mL) - or ATP (1 mmol/L) -mediated cytoplasmic Ca^{2+} concentrations were measured in Fura-2–loaded ECs by a fluorescence microscope (n=12 each). †$P<0.001$, *$P<0.001$ vs VEGF-stimulated $PYK2^{-/-}$ cells. B, Top, ECs were fixed with 4% paraformaldehyde 30 minutes after VEGF stimulation, treated with 0.05% triton, and immunostained with anti-NFATc2 antibodies and propidium iodide (PI). Bottom, PYK2-deficient ECs were transfected with GFP-tagged PYK2 plasmid. Forty-eight hours after transfection, cells were stimulated with VEGF for 30 minutes and immunostained with anti-NFATc2 and anti-GFP antibodies. The number of cells in which NFATc2 was translocated to the nucleus was counted and shown relative to total plated cell numbers (n=4 in each experiment). *$P<0.05$, **$P<0.005$ vs nonstimulated control cells. †$P<0.05$, ††$P<0.01$. Scale bar=10 μm. C, After serum starvation (0.5% FBS) for 16 hours, cells were preincubated with BAPTA-AM (5 μmol/L) in the Ca^{2+}-free medium for 45 minutes and subsequently stimulated by VEGF for 5 minutes. Lysates were subject to immunoblot by antibodies against Akt and ^{473}Ser-phosphorylated Akt.

wild-type aorta (from 32±8 to 18±3%; $P<0.005$; n=4). These findings indicate that Ach-mediated vasorelaxation depends mainly on NO production, in which an involvement of PYK2-mediated NO signaling was estimated to be ≈64% [(59−32/59−17)×100] of the total NO-mediated vasodilation activated downstream of Ach. NO donor (nitroprusside) –induced vasorelaxation of the aorta was similar in both groups (82±4 versus 83±4%; n=5), suggesting that NO-mediated signal transduction for vasodilatation is not impaired in the PYK2-deficient aorta (Figure 4C).

NO-mediated vasodilatation requires cGMP as a second messenger. We therefore measured the amount of cGMP in the aorta. Basal cGMP production in the $PYK2^{-/-}$ mice was 41% lower than that in the wild-type mice. Ach increased aortic cGMP production 4.8-fold in the wild-type mice, whereas the increase in the $PYK2^{-/-}$ mice was 2.0-fold, significantly ($P<0.01$) lower than in the wild-type mice (Figure 4D).

Decrease in Neovessel Formation by PYK2 Deficiency

Angiogenesis in the ischemic tissue requires eNOS activation.[17] We analyzed the blood flow recovery and neovessel formation after hind-limb ischemia. The ratio of blood flow recovery assessed by laser Doppler imaging was significantly lower in the $PYK2^{-/-}$ mice than in the wild-type mice (50% versus 76% recovery at 3 weeks after ischemia; $P<0.01$; Figure 5A). Oral administration of L-NAME (3 mmol/L in drinking water) significantly reduced the recovery ratio in the wild-type (from 76% to 62%; $P<0.05$) and $PYK2^{-/-}$ (from 50% to 37%; $P<0.05$) mice (Figure 5A). Considering that the recovery ratio of the L-NAME–treated wild-type mice (62%) is close to that of the $PYK2^{-/-}$ mice (50%), the blood flow recovery after hind-limb ischemia is considered to be regulated mainly by PYK2-mediated NO signaling. We also counted the number of $CD31^+$ vessels in the ischemic muscle. There was no significant difference in the basal vessel

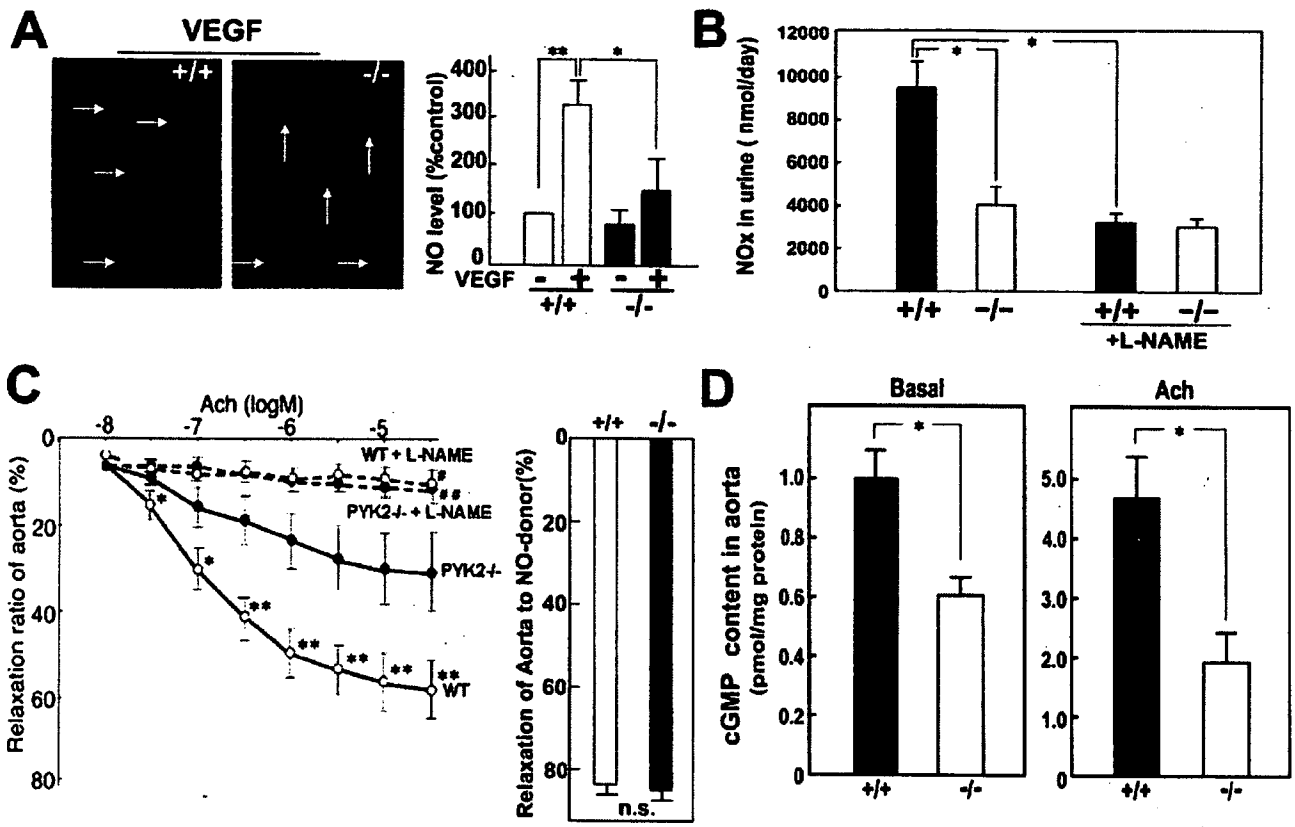

Figure 4. PYK2 effects on NO production and Ach-mediated vasodilatation. A, Measurement of the intracellular NO level. ECs were loaded with DAF-FM DA (10 μmol/L), and NO was visualized as green under laser microscopy. The average intensities in the ECs relative to the control group were evaluated. *P<0.01, **P<0.005 (n=8 each). B, NO production assessed by NO metabolites in the 24-hour urine sample was evaluated in the mice treated or untreated with L-NAME (3 mmol/L) for 7 days. Data are mean±SE (n=6). *P<0.005. C, Ach- and NO donor– (nitroprusside) mediated vasodilation in the aorta constricted by norepinephrine (100 nmol/L). Ach (10 nmol/L to 100 μmol/L) -mediated or nitroprusside (10 μmol/L) relaxation in the Tyrode's solution with or without L-NAME (10 μmol/L) was assessed by percent relaxation relative to papaverine (100 μmol/L) -mediated relaxation (100%). *P<0.05, **P<0.01 vs the same concentration of the PYK2$^{-/-}$ mice; #P<0.001 vs the maximum concentration of the wild-type mice; ##P<0.005 vs the maximum concentration of the PYK2$^{-/-}$ mice. D, cGMP contents in tissue lysates from untreated (basal) or Ach (1 μmol/L) -stimulated aorta were measured with an enzyme immunoassay kit. *P<0.01. Data are mean±SE (n=4 each); representative results are shown.

numbers surrounding the muscle fibers. The vessel number (per muscle fiber) in the wild-type mice increased 2.3-fold (P<0.005) after hind-limb ischemia, whereas the PYK2$^{-/-}$ mice showed no significant increase (Figure 5B).

We next examined whether PYK2 deficiency affects the mobilization or differentiation of EPCs. We found that 3 days after limb ischemia, the number of circulating CD45^{-}/Flk-1^{+} EPCs was significantly lower (36%; P<0.05) in the PYK2$^{-/-}$ mice than the wild-type mice (0.28±0.06% and 0.18±0.03% relative to total peripheral blood mononuclear cells, respectively; n=10 each; Figure 5C). Considering that the mobilization of EPCs was reportedly regulated by the eNOS function of EPCs in a VEGF-dependent manner,[18] the present study suggests that PYK2 deficiency attenuates VEGF-mediated EPC mobilization by impairing Ca^{2+}/eNOS signaling.

Impaired cGMP-Dependent Protein Kinase– and eNOS-Mediated Migration of PYK2-Deficient ECs

NO-mediated angiogenesis depends on the migration of ECs, in which cGMP-dependent protein kinase (GK) or eNOS plays a crucial role.[19] Because it was reported that the migration of macrophages was severely impaired in PYK2$^{-/-}$ mice,[11] the migration activity of aortic ECs was evaluated by the Boyden chamber assay. VEGF-mediated migration was 41% lower (P<0.01) in the PYK2-deficient ECs than wild-type ECs (Figure 6A). Pretreatment with L-NAME (3 mmol/L) or Rp-8-Br-cGMPS (1 μmol/L, a GK inhibitor) markedly inhibited the VEGF-mediated migration activities of wild-type ECs (50% and 45% inhibition, respectively; Figure 6A). L-Arginine (1 mmol/L) or GK activator 8-Bromo-cGMP (1 μmol/L) treatment restored the reduced migration of PYK2-deficient ECs to the wild-type level, whereas L-NAME or GK inhibitor (1 μmol/L) did not significantly affect their migration activities (Figure 6A).

The tubular formation activity and 3-dimensional angiogenesis in the Matrigel plug were significantly decreased in the PYK2-deficient ECs (59% and 38% decrease, respectively; Figure 6B and 6C). L-NAME diminished the tubular formation of wild-type ECs (39%; P<0.05), and L-arginine treatment improved the decreased activity of PYK2-deficient ECs (52%; P<0.01) (Figure 6B). These findings suggested that PYK2-mediated migration of ECs and angiogenic response are regulated mainly by NO and GK activation.

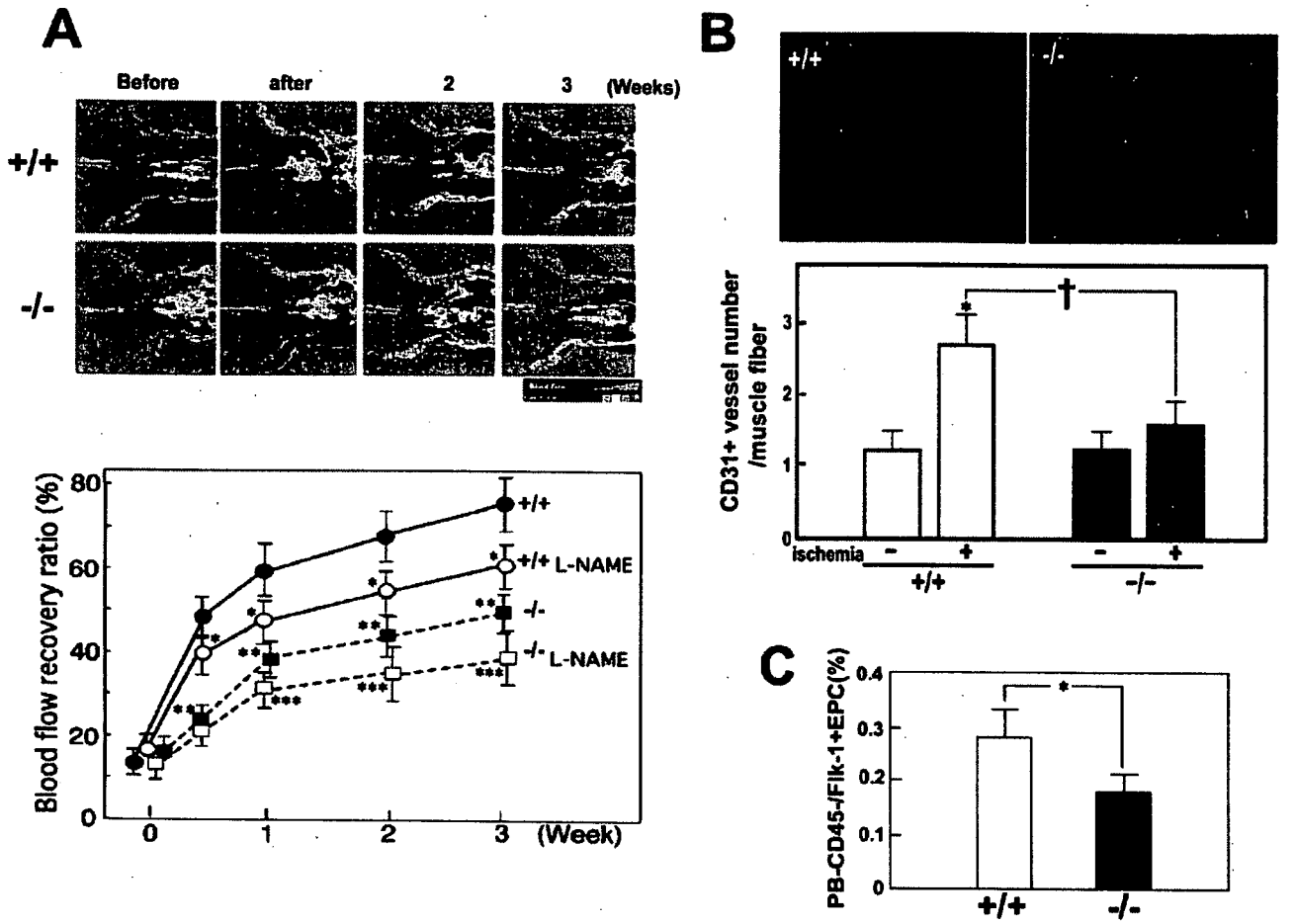

Figure 5. Reduced recovery of blood flow and neovessel formation in the ischemic hind limb of PYK2$^{-/-}$ mice. A, Reduced blood perfusion in ischemic limbs (green to blue) was observed in the PYK2$^{-/-}$ mice in contrast with perfusion (red to yellow) in the wild-type mice. Computer-assisted analyses revealed significantly lower blood perfusion values in PYK2$^{-/-}$ mice. Administration of L-NAME (3 mmol/L) in drinking water reduced the increased perfusion in both the wild-type and PYK2$^{-/-}$ mice. Values shown are mean±SE (n=8 each time point). *P<0.05, **P<0.01 vs wild-type mice; ***P<0.05 vs PYK2$^{-/-}$ mice. B, Hind-limb muscles were removed 14 days after ischemia, and ECs were immunostained with an anti-CD31 antibody. The number of CD31^{+} vessels surrounding the muscle fiber is shown. Data are mean±SE (n=8 each). *P<0.005 vs ischemia (-) muscles; †P<0.005. C, Three days after hind-limb ischemia, peripheral blood was incubated with FITC-conjugated anti-CD45 and PE-conjugated anti-Flk-1 antibodies. Peripheral blood–derived mononuclear cells were analyzed by fluorescence-activated cell sorter after lysis of erythrocytes. The relative number of CD45^{-}/Flk-1^{+} EPCs to total mononuclear cells was shown (n=10; *P<0.05).

Considering that GK affects the cytoskeleton structure,[20] PYK2 may modulate the cytoskeleton structure, leading to the regulation of cell migration and eventually angiogenesis. We therefore examined the effect of PYK2 on the F-actin structure of ECs. In the basal condition, we observed the stress fibers in 55±5% of the total wild-type ECs attaching on a fibronectin-coated dish and in 76±5% of PYK2-deficient ECs (P<0.05) (Figure 7A). VEGF stimulation markedly decreased the number of stress fiber–positive wild-type cells (from 55±5% to 15±4%; P<0.01) and 64±6% of the total attaching wild-type cells exhibited the accumulation of F-actin at the plasma membrane, whereas in the PYK2-deficient ECs, 72±8% of cells still had the apparent stress fibers and the cells showing the F-actin accumulation at the plasma membrane was only 23±3%. Pretreatment with L-NAME inhibited VEGF-mediated F-actin accumulation at the plasma membrane (P<0.01) and increased the stress fiber formation (P<0.05) in the wild-type cells, whereas the addition of L-arginine to PYK2-deficient ECs attenuated the stress fiber formation (P<0.01) and enhanced the VEGF-mediated F-actin accumulation at the plasma membrane (P<0.05).

Because F-actin structure was regulated by Rho-family small GTPases, we evaluated the activities of RhoA and Rac1 by pull-down assay using GST-RBD[21] and GST-PBD,[22] respectively (Figure 7B). The amount of GTP-bound RhoA was decreased significantly in the wild-type ECs 5 minutes after VEGF treatment, whereas in the PYK2-deficient ECs, they were reduced more extensively than in the wild-type ECs. In contrast, the amount of GTP-bound Rac1 was increased markedly in the wild-type ECs, whereas its increase was abolished by the PYK2 deficiency. Considering that Rac1 plays a pivotal role in F-actin reorganization[23] and PYK2 promotes Rac-mediated JNK activation,[24] lack of VEGF-mediated Rac1 activation may be associated with the altered F-actin structure in the PYK2-deficient cells. Further-

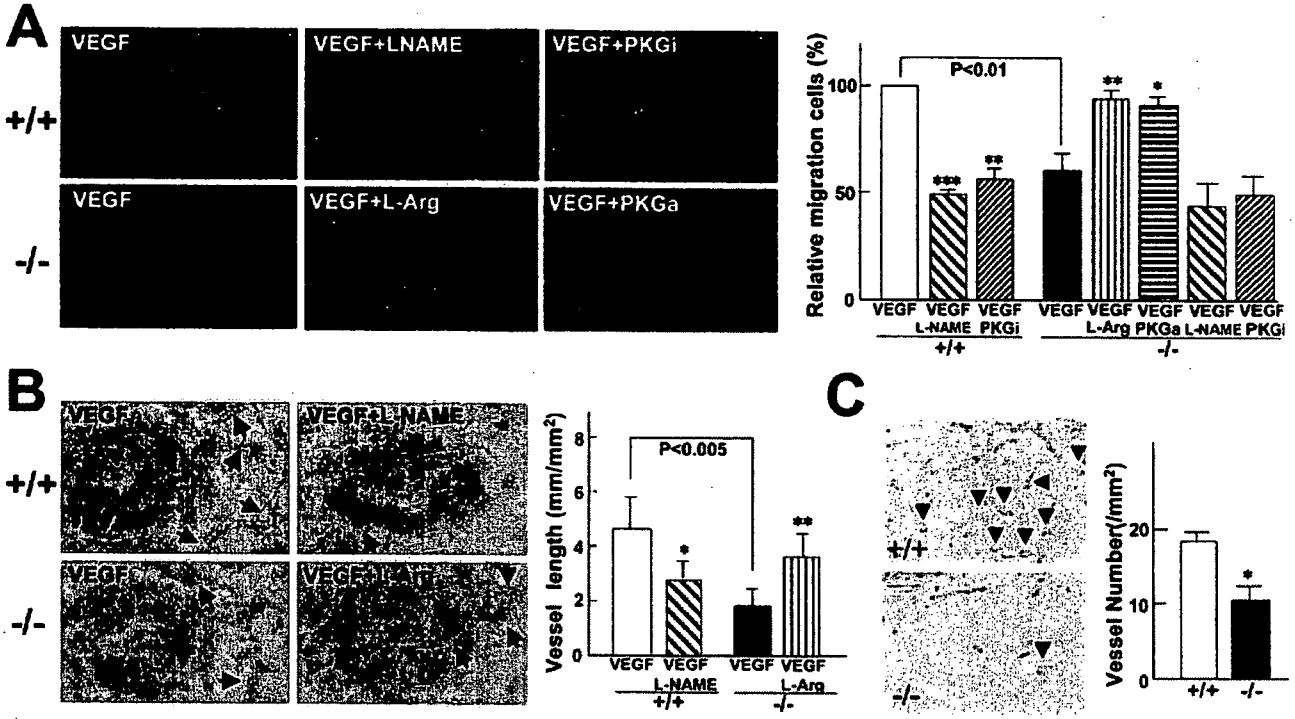

Figure 6. Decrease in GK- and eNOS-dependent migration of PYK2-deficient ECs. A, VEGF-mediated migration of ECs was evaluated with GK inhibitor (PKGi; 1 μmol/L Rp-8-Br-cGMPS), L-NAME (3 mmol/L), GK activator (PKGa; 1 μmol/L 8-Bromo-cGMP), and L-arginine (L-Arg; 1 mmol/L) using the modified Boyden chamber assay. The migrated cells were counted and arbitrarily expressed relative to VEGF-migrated wild-type ECs (100%). *$P<0.01$, **$P<0.005$, ***$P<0.001$ vs VEGF-treated control cells (n=5). B, Tubular formation of ECs was assessed with or without L-NAME (3 mmol/L) or L-Arg (1 mmol/L). Arrows indicates tubular formation. Total vessel lengths in the microscopic fields were evaluated (n=4 each). *$P<0.05$, **$P<0.01$ vs VEGF-treated control cells. C, Histological appearance (hematoxylin-eosin staining) of the Matrigel plug sections showing EC-forming vessels (arrowheads). The vessels were counted (n=6). *$P<0.01$.

more, treatment with L-NAME attenuated VEGF-mediated Rac1 activation in the wild-type ECs, whereas addition of L-arginine to the PYK2-deficient ECs restored the response, indicating that PYK2-mediated Rac1 activation is NO dependent (Figure 7B).

Taniyama et al[25] showed that in the angiotensin II–stimulated cells (vascular smooth muscle cells), Ca^{2+}-activated PYK2 acts as a scaffold for Src-dependent phosphorylation of 3-phosphoinositide-dependent protein kinase, the activator of Akt, whereas VEGF-induced Akt activation appears to be Ca^{2+} independent (Figure 3C). We therefore evaluated the target of PYK2 in the VEGF-mediated signaling pathways leading to Akt activation or Ca^{2+} mobilization. We found that VEGF stimulation causes PYK2 association with Src in the wild-type ECs, leading to the phosphorylation of Src (Figure 7C) and Akt (Figures 2B and 7C). PYK2 deficiency significantly inhibited VEGF-mediated Src and Akt activation, and inhibition of Src activity by PP1 blocked Akt and PYK2 phosphorylation (Figures 2B and 7C). Immunoprecipitation experiments indicated that Src, but not PYK2, is closely associated with the p85 subunit of PI3K and that the Src/PI3K complex binds to PYK2 in response to VEGF (Figure 7C, bottom).

To study PYK2-mediated Ca^{2+} signaling after stimulation with VEGF, we studied PLCγ1 activation, known to cause an increase in Ca^{2+} level.[26] We found that VEGF-mediated Src association with PLCγ1 and phosphorylation of ^{783}Tyr-PLCγ1 (both basal and VEGF induced) were significantly decreased in the PYK2-deficient cells and that the treatment with the Src inhibitor PP1 abolished VEGF-induced PLCγ1 phosphorylation (Figure 7D).

Taken together, it is likely that the direct target of PYK2 is Src and that Src-bound PI3-kinase and Src-bound PLCγ are involved in activation of Akt and Ca^{2+} mobilization, respectively.

Discussion

Tyrosine kinases have been assumed to be the upstream molecule for PI3K-Akt-eNOS or Ca^{2+}-eNOS pathways. eNOS is activated by Akt, and intracellular Ca^{2+} upregulates eNOS activity, raising the possibility that Ca^{2+}-dependent tyrosine kinase PYK2 is a possible eNOS activator. This study provides the first evidence that (1) PYK2 deficiency attenuates VEGF-mediated eNOS phosphorylation associated with decreased Akt activation and intracellular Ca^{2+} mobilization, (2) PYK2 is associated with the Src/PI3K complex and inhibition of Src blocked Akt phosphorylation, (3) Ach-mediated vasodilation of the aorta was diminished by decreased cGMP production in PYK2$^{-/-}$ mice, and (4) PYK2 plays a central role in VEGF- or ischemia-mediated eNOS activation followed by angiogenic response in which VEGF-induced EPC mobilization, VEGF-dependent migration, actin cytoskeletal reorganization associated with reduced Rac1 activation were markedly inhibited in the PYK2-deficient

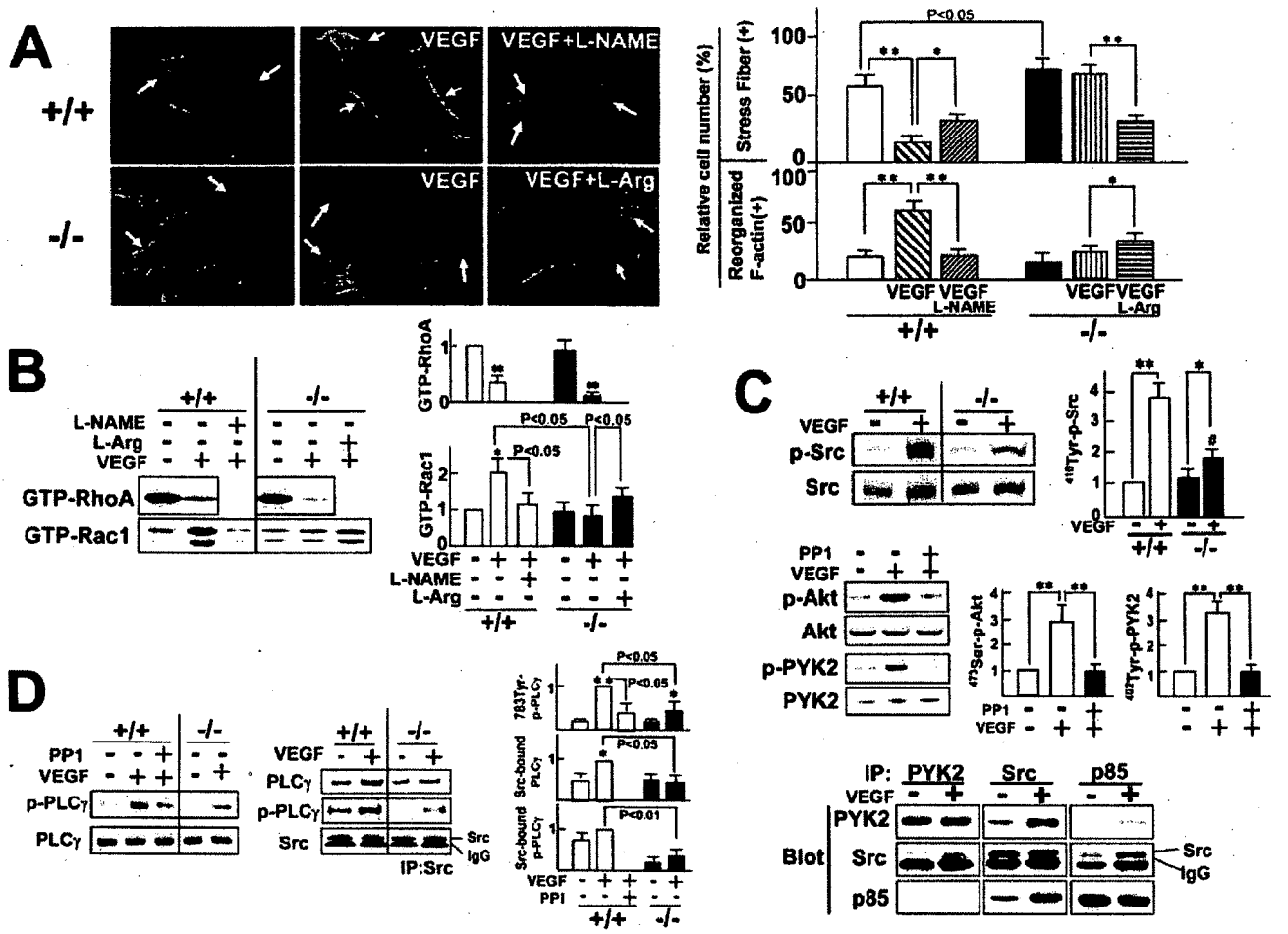

Figure 7. Impaired reorganization of F-actin in PYK2-deficient cells. A, F-actin structure of ECs. ECs were cultured on the fibronectin-coated glass chamber. After 16 hours of starvation (0.5% serum) with or without preincubation by L-arginine (1 mmol/L) or L-NAME (3 mmol/L), ECs were stimulated with VEGF (100 ng/mL) for 30 minutes, fixed with 4% paraformaldehyde, and permeabilized with 0.02% triton, and F-actin was stained with TRITC-labeled phalloidin. Representative staining was shown (n=7 each). Yellow arrows indicate the stress fiber; white arrows, accumulated F-actin at the plasma membrane. The cells with stress fiber or accumulated F-actin at the plasma membrane were counted, and the ratio (%) relative to total attaching cells was shown. *$P<0.05$, **$P<0.01$. B, Measurement of the VEGF-induced RhoA:GTP/Rac1:GTP. After 16 hours of starvation with or without L-NAME or L-arginine, ECs were incubated by VEGF for 5 minutes. Cell lysates were incubated with GST-RBD (Rho-binding domain) and GST-PBD (p21-binding domain) bound to glutathione beads as described in the Methods section of the online Data Supplement. The amount of RhoA:GTP and Rac1:GTP complex was determined by immunoblot with anti-RhoA and anti-Rac1 antibodies. *$P<0.05$, **$P<0.01$ (n=4 each) vs non-stimulated group. C, After 16 hours of starvation with or without PP1, ECs were incubated with VEGF for 5 minutes. Top, Cell lysates were subjected to Western blotting with antibodies against anti-^{416}Tyr-phosphorylated-Src or Src. Middle, Cell lysates of the wild-type ECs were analyzed by Western blotting with antibodies against Akt, ^{473}Ser-phosphorylated Akt, PYK2, and ^{402}Tyr-phosphorylated PYK2. Bottom, Cell lysates of the wild-type ECs were immunoprecipitated (IP), followed by Western blotting using antibodies against anti-PYK2, Src, and p85 subunit of PI3-kinase. *$P<0.05$, **$P<0.005$ (n=5 each experiment). D, After 16 hours of starvation with or without PP1, ECs were stimulated with VEGF for 5 minutes. Cell lysates were subjected to immunoblotting with antibodies against PLCγ1 or ^{783}Tyr-phosphorylated PLCγ1, plus immunoprecipitation with anti-Src antibody, followed by immunoblot with antibodies against PLCγ1, ^{783}Tyr-phosphorylated PLCγ1, or Src. *$P<0.05$, **$P<0.005$ (n=4 each) vs nonstimulated groups. #$P<0.05$ vs VEGF-stimulated wild-type ECs.

ECs. Cell migration reportedly requires the recycled mobilization of actin from the old focal adhesion toward the plasma membrane of the leading edge to form the lamellipodia and new focal contact,[27] suggesting that impaired reorganization of the F-actin at the plasma membrane plausibly causes attenuated migration of the PYK2-deficient ECs.

eNOS activation is dependent on an increase in $[Ca^{2+}]i$ and the binding of Ca^{2+}/calmodulin to the enzyme, leading to conformational change to displace the autoinhibitory loop.[28] If Ca^{2+} mobilization is totally abolished, administration of the eNOS substrate arginine could not restore eNOS activity. However, VEGF-induced increase in $[Ca^{2+}]i$ and subsequent translocation of NFATc2 in PYK2-deficient ECs remain ≈23% and ≈32%, respectively, of the wild-type cells (Figure 3). This increase in $[Ca^{2+}]i$ could cause the conformational change in eNOS, resulting in the recovery in eNOS activation after arginine administration.

The present study showed that PYK2 deficiency attenuates VEGF-mediated association of Src with PLCγ1 and phosphorylation of PLCγ1. VEGF was shown to stimulate the

association of VEGF receptor-2 with Src, and subsequent Src activation was a requisite for VEGF-mediated PLCγ1 activation.[29] Taken together, it is conceivable that the lack of intracellular Ca^{2+} mobilization in VEGF-stimulated PYK2-deficient cells is due to the inhibition of Src-associated PLCγ activation.

Src and PYK2 are mutually activated in a stepwise manner. Association of Src-SH2-domain with ^{402}Tyr-phosphorylated-PYK2 leads to conformational change in Src to release the internal autoinhibition, resulting in the upregulation of its activity. Conversely, activated Src phosphorylates ^{881}Tyr-PYK2, leading to the downstream Grb2/Ras/MAPK pathway.[10] In response to VEGF receptor-2 stimulation, Src binds toward the phosphorylated ^{1212}Tyr of VEGF receptor-2 with its SH2 domain, leading to Src activation.[30] In addition, VEGF promotes association of VEGF receptor-2 with integrin ($\alpha V\beta 3$) and transmits integrin-dependent cell biological responses.[31] Activation of integrin ($\alpha V\beta 3$) induces phosphorylation of ^{402}Tyr-PYK2 and its association with integrin $\beta 3$.[32] Integrin-activated PYK2 is associated with Src[33] and involved in VEGF-mediated cell migration.[34] Furthermore, integrin ($\alpha V\beta 5$) plays a crucial role in angiogenesis,[35] and inhibition of integrin ($\alpha V\beta 5$) disrupted VEGF-mediated and Src-dependent angiogenesis.[36] Thus, PYK2/Src complex is likely to integrate integrin with the VEGF receptor-2 signaling system.

Fluid shear stress–mediated activation of eNOS is dependent on Ca^{2+} mobilized through a mechanical stress–activated Ca^{2+} channel on the plasma membrane, whereas a Ca^{2+}-independent system has been reported recently. Fleming et al[37] demonstrated that shear stress elicits Src-mediated phosphorylation of platelet EC adhesion molecule-1 (PECAM-1) at the cell-to-cell contact, which is crucial for subsequent activation of Akt and eNOS. Furthermore, Tzima et al[38] showed that PECAM-1 forms a mechanosensory complex with VEGF receptor-2, leading to activation of PI3-kinase. These findings suggest that VEGF receptor-2 is involved in Src/PECAM-1–mediated Akt/eNOS activation in Ca^{2+}-independent manner. Unlike PECAM-1, PYK2 is localized at the cell-to–extracellular-matrix contact region.[8,33] VEGF promotes the association of VEGF receptor-2 with integrin and integrin-dependent cell biological responses.[31] Thus, the PYK2/Src complex transmits the VEGF signals in association with extracellular matrix/integrins, suggesting that the Ca^{2+}-independent Src/PECAM-1 system is unlikely to be involved in PYK2-mediated Src activation.

Because the blood flow recovery ratio in the ischemic limbs was increased ≈5-fold on day 7 compared with the day 0 control level (Figure 5A), hemodynamic shear stress also could be proportionally elevated in the newly formed vessels. Shear stress was shown to elicit the phosphorylation of ^{1177}Ser-eNOS by activating both Akt and PKA.[28] As shown in Figure 2A, Akt, AMPK, and PKA showed peak phosphorylation on day 1 and at 2 hours, respectively, and then PKA and AMPK reversed to the baseline level on day 7, whereas moderate activation of Akt was observed on day 7 (210% increase compared with the basal level), suggesting that Akt, rather than PKA and AMPK, is involved in the eNOS activation 7 days after limb ischemia. However, further studies are required to define the involvement of other kinases associated with flow shear stress.

Conclusions

This analysis of $PYK2^{-/-}$ mice demonstrates the critical role of PYK2 in Akt/NO signals activated by vasoactive substances or ischemic stress that modulates the vascular tonus or angiogenesis. These findings indicate that PYK2 can operate as a modulator for extracellular versatile stimuli, leading to eNOS activation, and is closely involved in the receptor- or ischemia-activated NO signaling events and thus regulates the cytoskeleton structure, vasoreactive function, or angiogenic response.

Acknowledgment

The authors profoundly appreciate Dr Nobuo Shirahashi for his advice and help with the statistical analysis.

Source of Funding

This work was supported by grants from the Ministry of Education, Culture, Sports, Science and Technology of Japan (grants 13670763 and 15590778 to Dr Okigaki).

Disclosures

None.

References

1. Shesely EG, Maeda N, Kim HS, Desai KM, Krege JH, Laubach VE, Sherman PA, Sessa WC, Smithies O. Elevated blood pressures in mice lacking endothelial nitric oxide synthase. *Proc Natl Acad Sci U S A*. 1996;93:13176–13181.
2. Fukumura D, Gohongi T, Kadambi A, Izumi Y, Ang J, Yun CO, Buerk DG, Huang PL, Jain RK. Predominant role of endothelial nitric oxide synthase in vascular endothelial growth factor-induced angiogenesis and vascular permeability. *Proc Natl Acad Sci U S A*. 2001;98:2604–2609.
3. Fulton D, Gratton JP, McCabe TJ, Fontana J, Fujio Y, Walsh K, Franke TF, Papapetropoulos A, Sessa WC. Regulation of endothelium-derived nitric oxide production by the protein kinase Akt. *Nature*. 1999;399:597–601.
4. Dimmeler S, Fleming I, Fisslthaler B, Hermann C, Busse R, Zeiher AM. Activation of nitric oxide synthase in endothelial cells by Akt-dependent phosphorylation. *Nature*. 1999;399:601–605.
5. Haynes MP, Li L, Sinha D, Russell KS, Hisamoto K, Baron R, Collinge M, Sessa WC, Bender Jr. Src kinase mediates phosphatidylinositol 3-kinase/Akt-dependent rapid endothelial nitric-oxide synthase activation by estrogen. *J Biol Chem*. 2003;278:2118–2123.
6. Lev, S. Moreno H, Martinez R, Canoll P, Peles E, Musacchio JM, Plowman GD, Rudy B, Schlessinger J. Protein tyrosine kinase PYK2 involved in Ca(2+)-induced regulation of ion channel and MAP kinase functions. *Nature*. 1995;376:737–745.
7. Yu H, Marchetto GS, Dy R, Hunter D, Calvo B, Dawson TL, Wilm M, Anderegg RJ, Graves LM, Earp HS. Activation of a novel calcium-dependent protein-tyrosine kinase: correlation with c-Jun N-terminal kinase but not mitogen-activated protein kinase activation. *J Biol Chem*. 1996;271:29993–29998.
8. Astier A, Avraham H, Manie SN, Groopman J, Canty T, Avraham S, Freedman AS. The related adhesion focal tyrosine kinase is tyrosine-phosphorylated after beta1-integrin stimulation in B cells and binds to p^{130cas}. *J Biol Chem*. 1997;272:228–232.
9. Tian D, Litvak V, Lev S. Cerebral ischemia and seizures induce tyrosine phosphorylation of PYK2 in neurons and microglial cells. *J Neurosci*. 2000;20:6478–6487.
10. Dikic I, Tokiwa G, Lev S, Courtneidge SA, Schlessinger J. A role for Pyk2 and Src in linking G-protein-coupled receptors with MAP kinase activation. *Nature*. 1996;383:547–550.
11. Okigaki M, Davis C, Falasca M, Harroch S, Felsenfeld D, Sheetz MP, Schlessinger J. Pyk2 regulates multiple signaling events crucial for macrophage morphology and migration. *Proc Natl Acad Sci U S A*. 2003;100:10740–10745.

12. Tamarat R, Silvestre JS, Kubis N, Benessiano J, Duriez M, deGasparo M, Henrion D, Levy BI. Endothelial nitric oxide synthase lies downstream from angiotensin II-induced angiogenesis in ischemic hindlimb. *Hypertension*. 2002;39:830–835.
13. Michell BJ, Chen Z, Tiganis T, Stapleton D, Katsis F, Power DA, Sim AT, Kemp BE. Coordinated control of endothelial nitric-oxide synthase phosphorylation by protein kinase C and the cAMP-dependent protein kinase. *J Biol Chem*. 2001;276:17625–17628.
14. Boo YC, Sorescu G, Boyd N, Shiojima I, Walsh K, Du J, Jo H. Shear stress stimulates phosphorylation of endothelial nitric-oxide synthase at Ser1179 by Akt-independent mechanisms: role of protein kinase A. *J Biol Chem*. 2002;277:3388–3396.
15. Yamamoto K, Sokabe T, Matsumoto T, Yoshimura K, Shibata M, Ohura N, Fukuda T, Sato T, Sekine K, Kato S, Isshiki M, Fujita T, Kobayashi M, Kawamura K, Masuda H, Kamiya A, Ando J. Impaired flow-dependent control of vascular tone and remodeling in P2X4-deficient mice. *Nat Med*. 2006;12:133–137.
16. Hernandez GL, Volpert OV, Iniguez MA, Lorenzo E, Martinez-Martinez S, Grau R, Fresno M, Redondo JM. Selective inhibition of vascular endothelial growth factor-mediated angiogenesis by cyclosporin A: roles of the nuclear factor of activated T cells and cyclooxygenase 2. *J Exp Med*. 2001;193:607–620.
17. Murohara T, Asahara T, Silver M, Bauters C, Masuda H, Kalka C, Kearney M, Chen D, Symes JF, Fishman MC, Huang PL, Isner JM. Nitric oxide synthase modulates angiogenesis in response to tissue ischemia. *J Clin Invest*. 1998;101:2567–2578.
18. Aicher A, Heeschen C, Mildner-Rihm C, Urbich C, Ihling C, Technau-Ihling K, Zeiher AM, Dimmeler S. Essential role of endothelial nitric oxide synthase for mobilization of stem and progenitor cells. *Nat Med*. 2003;9:1370–1376.
19. Smolenski A, Poller W, Walter U, Lohmann SM. Regulation of human endothelial cell focal adhesion sites and migration by cGMP-dependent protein kinase I. *J Biol Chem*. 2000;275:25723–25732.
20. Surks HK, Mochizuki N, Kasai Y, Georgescu SP, Tang KM, Ito M, Lincoln TM, Mendelsohn ME. Regulation of myosin phosphatase by a specific interaction with cGMP- dependent protein kinase Ialpha. *Science*. 1999;286:1583–1587.
21. Ren XD, Kiosses WB, Schwartz MA. Regulation of the small GTP-binding protein Rho by cell adhesion and the cytoskeleton. *EMBO J*. 1999;18:578–585.
22. Benard V, Bohl BP, Bokoch GM. Characterization of Rac and Cdc42 activation in chemoattractant-stimulated human neutrophils using a novel assay for active GTPases. *J Biol Chem*. 1999;274:13198–13204.
23. Ridley AJ, Hall A. The small GTP-binding protein rho regulates the assembly of focal adhesions and actin stress fibers in response to growth factors. *Cell*. 1992;70:389–399.
24. Tokiwa G, Dikic I, Lev S, Schlessinger J. Activation of Pyk2 by stress signals and coupling with JNK signaling pathway. *Science*. 1996;273:792–794.
25. Taniyama Y, Weber DS, Rocic P, Hilenski L, Akers ML, Park J, Hemmings BA, Alexander RW, Griendling KK. Pyk2- and Src-dependent tyrosine phosphorylation of PDK1 regulates focal adhesions. *Mol Cell Biol*. 2003;23:8019–8029.
26. Carroll DJ, Ramarao CS, Mehlmann LM, Roche S, Terasaki M, Jaffe LA. Calcium release at fertilization in starfish eggs is mediated by phospholipase Cgamma. *J Cell Biol*. 1997;138:1303–1311.
27. Lawson MA, Maxfield FR. Ca^{2+}- and calcineurin-dependent recycling of an integrin to the front of migrating neutrophils. *Nature*. 1995;377:75–79.
28. Fleming I, Busse R. Molecular mechanisms involved in the regulation of the endothelial nitric oxide synthase. *Am J Physiol Regul Integr Comp Physiol*. 2003;284:R1–R12.
29. He H, Venema VJ, Gu X, Venema RC, Marrero MB, Caldwell RB. Vascular endothelial growth factor signals endothelial cell production of nitric oxide and prostacyclin through flk-1/KDR activation of c-Src. *J Biol Chem*. 1999;274:25130–25135.
30. Meyer RD, Dayanir V, Majnoun F, Rahimi N. The presence of a single tyrosine residue at the carboxyl domain of vascular endothelial growth factor receptor-2/FLK-1 regulates its autophosphorylation and activation of signaling molecules. *J Biol Chem*. 2002;277:27081–27087.
31. Soldi R, Mitola S, Strasly M, Defilippi P, Tarone G, Bussolino F. Role of alphavbeta3 integrin in the activation of vascular endothelial growth factor receptor-2. *EMBO J*. 1999;18:882–892.
32. Butler B, Blystone SD. Tyrosine phosphorylation of beta3 integrin provides a binding site for Pyk2. *J Biol Chem*. 2005;280:14556–14562.
33. Duong LT, Lakkakorpi PT, Nakamura I, Machwate M, Nagy RM, Rodan GA. PYK2 in osteoclasts is an adhesion kinase, localized in the sealing zone, activated by ligation of alpha (v) beta3 integrin, and phosphorylated by src kinase. *J Clin Invest*. 1998;102:881–892.
34. Avraham HK, Lee TH, Koh Y, Kim TA, Jiang S, Sussman M, Samarel AM, Avraham S. Vascular endothelial growth factor regulates focal adhesion assembly in human brain microvascular endothelial cells through activation of the focal adhesion kinase and related adhesion focal tyrosine kinase. *J Biol Chem*. 2003;278:36661–36668.
35. Friedlander M, Brooks PC, Shaffer RW, Kincaid CM, Varner JA, Cheresh DA. Definition of two angiogenic pathways by distinct alpha v integrins. *Science*. 1995;270:1500–1502.
36. Hood JD, Frausto R, Kiosses WB, Schwartz MA, Cheresh DA. Differential alphav integrin-mediated Ras-ERK signaling during two pathways of angiogenesis. *J Cell Biol*. 2003;162:933–943.
37. Fleming I, Fisslthaler B, Dixit M, Busse R. Role of PECAM-1 in the shear-stress-induced activation of Akt and the endothelial nitric oxide synthase (eNOS) in endothelial cells. *J Cell Sci*. 2005;118:4103–4111.
38. Tzima E, Irani-Tehrani M, Kiosses WB, Dejana E, Schultz DA, Engelhardt B, Cao G, DeLisser H, Schwartz MA. A mechanosensory complex that mediates the endothelial cell response to fluid shear stress. *Nature*. 2005;437:426–431.

CLINICAL PERSPECTIVE

Although endothelial dysfunction causes atherosclerosis or vascular aging, drugs to improve endothelial functions have not been developed. Nitric oxide (NO) plays pivotal roles in the maintenance of endothelial function and vascular homeostasis, including vasodilatation, antiinflammatory effect, anticoagulation, antiproliferative effect of vascular smooth muscle cells, angiogenesis, and vasculogenesis. NO is produced by endothelial NO synthase (eNOS); therefore, a drug that upregulates eNOS function may improve endothelial function. For this purpose, it is important to clarify the molecular mechanism to activate eNOS. In the present study, we showed that tyrosine kinase PYK2 plays a crucial role in eNOS activation. Both PYK2 and eNOS are activated by hemodynamic mechanical stress, ischemic stress, and stimulation with endothelial growth factors, and PYK2 transmits calcium and Akt signaling pathways, both of which activate eNOS, suggesting that the drug developed to activate PYK2 may be feasible therapy for maintaining vascular homeostasis in various stress conditions. However, PYK2 also is involved in angiotensin II–mediated signaling to induce atherosclerosis, including vasoconstriction, vascular inflammation, and proliferation of vascular smooth muscle cells, indicating that PYK2 has dual effects on vascular function. The role of PYK2 in the maintenance of vascular homeostasis should be investigated further.

Circulation Research

JOURNAL OF THE AMERICAN HEART ASSOCIATION

American Heart Association®

Learn and Live℠

New Targeted Angiogenic Strategy: Bursting Bubbles

Tomosaburo Takahashi and Hiroaki Matsubara

Circ. Res. 2007;101;232-233
DOI: 10.1161/CIRCRESAHA.107.158253
Circulation Research is published by the American Heart Association. 7272 Greenville Avenue, Dallas, TX 72514
 Print ISSN: 0009-7330. Online ISSN: 1524-4571

See related article, pages 295–303

New Targeted Angiogenic Strategy
Bursting Bubbles

Tomosaburo Takahashi, Hiroaki Matsubara

Although recent procedural advances in revascularization such as percutaneous coronary intervention and coronary artery bypass grafting improve quality of life and prognosis of the patients with ischemic diseases, these is still a subset of patients who are refractory to these conventional therapies and have poor prognosis. Therapeutic angiogenesis might offer a novel approach to these patients. Therapeutic angiogenesis involves an intervention to induce the formation of new blood vessels to restore the arterial blood and oxygen supply to ischemic tissues.[1] Here, the term "angiogenesis" represents the process of new blood vessel formation in general (although the same term is also used to describe a more specific biological process in which the new capillaries sprout from preexisting vessels).

Evolving knowledge of mechanisms of new blood vessel formation has raised the expectations for therapeutic angiogenesis as a treatment option. Recent studies have identified many angiogenic growth factors, vascular transcription factors, and the cells involved in neovascularization.[1,2] Current potential strategies for therapeutic angiogenesis include delivering an angiogenic factor as a protein or a gene, and supplying cells which themselves are vascular progenitors or are releasing angiogenic factors. These strategies have worked in animal studies and in initial small scale open-labeled clinical trials. However, in larger, double-blinded controlled trials, therapeutic angiogenesis approaches have failed to show clinical benefits.[1,2] Why? Perhaps there are subtle differences in angiogenesis between animals and humans, or the ischemic pathophysiology of animal models and human diseases are dissimilar. Another possibility is technical difficulties in translating the biology into the practice.

In this issue of *Circulation Research*, Leon-Poi and colleagues report that targeted delivery of vascular endothelial growth factor (VEGF) gene using ultrasound-mediated destruction of cationic lipid microbubbles restores microvascular blood flow in a rat model of chronic hindlimb ischemia.[3] Ultrasound-targeted microbubble destruction uses ultrasound contrast agents, mostly perfluorocarbon bubbles stabilized with albumin or a lipid shell. When insonified at high acoustic power, these agents oscillate, resulting in microbubble disintegration.[4,5] This microbubble destruction has been shown to induce biophysical effects in the vicinity of contrast agents, and the therapeutic use of this phenomenon has been proposed for delivery of genes or drugs, and direct mechanical effects. One of the advantages of this method is that these bubbles cross the pulmonary circulation, so that the agents can be administrated intravenously, and reach any part of the body with arterial blood supply. And, at the desired sites, the agents can be activated or delivered by ultrasound. Leon-Poi et al coated the microbubbles with VEGF-expressing plasmid, intravenously administrated these bubbles, and then transferred the gene at the site of ischemia with ultrasound in hindlimb ischemia model.[3] This model of ischemia is chronic, because the gene was transferred 14 days after common iliac artery ligation.

Leon-Poi et al observed a significant increase in tissue perfusion mainly through the process of arteriogenesis, rather than angiogenesis in a narrow sense.[3] Arteriogenesis refers to the maturation or de novo synthesis of collateral vessels. The effect of VEGF gene transfer with this method on arteriogenesis rather than angiogenesis is intriguing, as remodeling or development of collaterals could be much more effective than an increase in capillary bed to restore the blood flow in the setting of flow-limiting proximal conduit artery lesions. It will be an important issue to determine whether the preferential effect on arteriogenesis is associated with the method of gene delivery, ultrasonic destruction of microbubble destruction (Figure).

Although the gene delivery is an important application of ultrasound-mediated microbubble destruction,[4–6] use of this method is not limited to gene therapy. Acoustic cavitation leads to microbubble oscillation and collapse. Electron microscopic analysis showed transient pore formation on cell membrane immediately after microbubble destruction, called sonoporation.[4,5] These mechanical effects facilitate entry of gene into the cells. At the same time, these mechanical forces affect nearby cells and tissues in vicinity of microbubble destruction. For example, microbubble destruction can facilitate thrombolysis in combination with thrombolytic agents such as urokinase and tissue plasminogen activator.[7,8] Furthermore, ultrasound-mediated microbubble destruction itself can be angiogenic, as ultrasound-mediated microbubble destruction has been shown to be able to induce capillary rupture and increase the density of arterioles in ischemic muscle with local recruitment of VEGF producing inflammatory cells.[9,10] Although capillary rupture with higher energies of ultrasound is just a step from adverse tissue damage, even with ultrasound without capillary rupture, ultrasound-mediated microbubble destruction has direct effects on vasculature and surrounding tissues. These effects can be

From the Department of Cardiovascular Medicine (T.T., H.M.), Kyoto Prefectural University of Medicine, Kyoto, Japan; Department of Experimental Therapeutics (T.T., H.M.), Translational Research Center, Kyoto University Hospital, Kyoto, Japan.

Correspondence to Tomosaburo Takahashi, Department of Cardiovascular Medicine, Kyoto Prefectural University of Medicine, 465 Kajii-cho Kawaramachi-Hirokoji, Kamigyo-ku, Kyoto 602-8566, Japan. E-mail ttaka@koto.kpu-m.ac.jp

(*Circ Res.* 2007;101:232-233.)

***Circulation Research* is available at http://circres.ahajournals.org**
DOI: 10.1161/CIRCRESAHA.107.158253

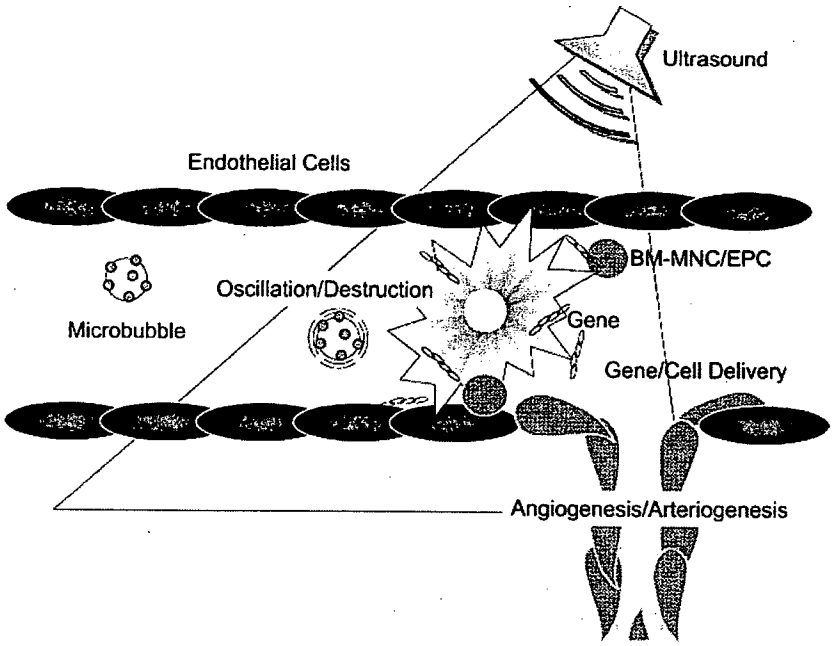

Schematic diagram of ultrasound-mediated microbubble destruction. Microbubbles enclosing therapeutic agents such as genes or drugs reach the local sites through circulation. At the desired site, ultrasound is applied, which oscillates and collapses the microbubbles, leading to direct biophysical effects on tissue or the delivery of therapeutic agents.

used for potential therapies, especially when combined with other modalities. One such example is microbubble destruction in combination with cell therapy. We have shown that targeted delivery of bone marrow-derived mononuclear cells by ultrasound-mediated microbubble destruction significantly enhances angiogenic response both in an ischemic hindlimb model and in a δ-sarcoglycan deficient cardiomyopathy model.[11,12] In the ischemic hindlimb model, ultrasound-mediated microbubble destruction induces platelet activation on the surface of endothelium, and subsequent induction of adhesion molecules on endothelium, which in turn stimulates recruitment of angiogenic mononuclear cells and enhances new vessel formation.[11] Ultrasound-mediated targeted cardiac delivery of marrow-derived mononuclear cells also efficiently enhances regional blood flow in myopathic hamsters, leading to improvement of cardiac function.[12]

Recent proof-of-principal studies show that ultrasound-mediated microbubble destruction has great potential to target various substrates including genes, proteins, drugs and cells to the desired sites. However, before this strategy is adopted in the clinic, many issues have to be resolved. Which patients are ideal subjects? What tissues are ideal target locations? What proteins and cells are ideal substrates to be delivered by microbubbles? Furthermore, technical issues of ultrasound-mediated microbubble destruction such as microbubble composition and ultrasound application must be refined. More collaboration between clinicians, biologist, chemists and engineers is needed to bring this exciting technique into the clinic.

Sources of Funding

This work was supported by Grants-in-Aid from the Ministry of Education, Culture, Sports, Science and Technology of Japan, and Grants-in-Aid from the Ministry of Health, Labor, and Welfare of Japan.

Disclosures

None.

References

1. Simons M. Angiogenesis: where do we stand now? *Circulation.* 2005; 111:1556–1566.
2. Shantsila E, Watson T, Lip GY. Endothelial progenitor cells in cardiovascular disorders. *J Am Coll Cardiol.* 2007;49:741–752.
3. Leong-Poi H, Kuliszewski MA, Lekas M, Sibbald M, Teichert-Kuliszewska K, Klibanov AL, Stewart DJ, Lindner JR. Therapeutic Arteriogenesis by Ultrasound-Mediated Vegf165 Plasmid Gene Delivery to Chronically Ischemic Skeletal Muscle. *Circ Res.* 2007;101:295–303.
4. Bekeredjian R, Grayburn PA, Shohet RV. Use of ultrasound contrast agents for gene or drug delivery in cardiovascular medicine. *J Am Coll Cardiol.* 2005;45:329–335.
5. Newman CM, Bettinger T. Gene therapy progress and prospects: ultrasound for gene transfer. *Gene Ther.* 2007;14:465–475.
6. Kondo I, Ohmori K, Oshita A, Takeuchi H, Fuke S, Shinomiya K, Noma T, Namba T, Kohno M. Treatment of acute myocardial infarction by hepatocyte growth factor gene transfer: the first demonstration of myocardial transfer of a "functional" gene using ultrasonic microbubble destruction. *J Am Coll Cardiol.* 2004;44:644–653.
7. Mizushige K, Kondo I, Ohmori K, Hirao K, Matsuo H. Enhancement of ultrasound-accelerated thrombolysis by echo contrast agents: dependence on microbubble structure. *Ultrasound Med Biol.* 1999;25:1431–1437.
8. Tachibana K, Tachibana S. Albumin microbubble echo-contrast material as an enhancer for ultrasound accelerated thrombolysis. *Circulation.* 1995;92:1148–1150.
9. Song J, Qi M, Kaul S, Price RJ. Stimulation of arteriogenesis in skeletal muscle by microbubble destruction with ultrasound. *Circulation.* 2002; 106:1550–1555.
10. Yoshida J, Ohmori K, Takeuchi H, Shinomiya K, Namba T, Kondo I, Kiyomoto H, Kohno M. Treatment of ischemic limbs based on local recruitment of vascular endothelial growth factor-producing inflammatory cells with ultrasonic microbubble destruction. *J Am Coll Cardiol.* 2005;46:899–905.
11. Imada T, Tatsumi T, Mori Y, Nishiue T, Yoshida M, Masaki H, Okigaki M, Kojima H, Nozawa Y, Nishiwaki Y, Nitta N, Iwasaka T, Matsubara H. Targeted delivery of bone marrow mononuclear cells by ultrasound destruction of microbubbles induces both angiogenesis and arteriogenesis response. *Arterioscler Thromb Vasc Biol.* 2005;25:2128–2134.
12. Zen K, Okigaki M, Hosokawa Y, Adachi Y, Nozawa Y, Takamiya M, Tatsumi T, Urao N, Tateishi K, Takahashi T, Matsubara H. Myocardium-targeted delivery of endothelial progenitor cells by ultrasound-mediated microbubble destruction improves cardiac function via an angiogenic response. *J Mol Cell Cardiol.* 2006;40:799–809.

KEY WORDS: therapeutic angiogenesis ■ gene therapy ■ ultrasound ■ microbubbles

Circ J 2007; **71:** 1199–1207

Intracoronary Transplantation of Non-Expanded Peripheral Blood-Derived Mononuclear Cells Promotes Improvement of Cardiac Function in Patients With Acute Myocardial Infarction

Tetsuya Tatsumi, MD; Eishi Ashihara, MD††; Toshihide Yasui, MD; Shinsaku Matsunaga, MD; Atsumichi Kido, MD; Yuji Sasada, MSc*; Satoshi Nishikawa, MSc**; Mitsuyoshi Hadase, MD; Masahiro Koide, MD; Reo Nakamura, MD; Hidekazu Irie, MD; Kazuki Ito, MD; Akihiro Matsui, MD; Hiroyuki Matsui, MD; Maki Katamura, MD; Shigehiro Kusuoka, MD; Satoaki Matoba, MD; Satoshi Okayama, MD‡; Manabu Horii, MD‡; Shiro Uemura, MD‡; Chihiro Shimazaki, MD†; Hajime Tsuji, MD*; Yoshihiko Saito, MD‡; Hiroaki Matsubara, MD

Background Transplantation of non-expanded peripheral blood mononuclear cells (PBMNCs) enhances neovessel formation in ischemic myocardium and limbs by releasing angiogenic factors. This study was designed to examine whether intracoronary transplantation of PBMNCs improves cardiac function after acute myocardial infarction (AMI).

Methods and Results After successful percutaneous coronary intervention (PCI) for a ST-elevation AMI with occlusion of proximal left anterior descending coronary artery within 24 h, patients were assigned to either a control group or the PBMNC group that received intracoronary infusion of PBMNCs within 5 days after PCI. PBMNCs were obtained from patients by COBE spectra-apheresis and concentrated to 10 ml, 3.3 ml of which was infused via over-the-wire catheter. The primary endpoint was the global left ventricular ejection fraction (LVEF) change from baseline to 6 months' follow-up. The data showed that the absolute increase in LVEF was 7.4% in the control group and 13.4% (p=0.037 vs control) in the PBMNC group. Cell therapy resulted in a greater tendency of ΔRegional ejection fraction (EF) or significant improvement in the wall motion score index and Tc-99m-tetrofosmin perfusion defect score associated with the infarct area, compared with controls. Moreover, intracoronary administration of PBMNCs did not exacerbate either left ventricular (LV) end-diastolic and end-systolic volume expansion or high-risk arrhythmia, without any adverse clinical events.

Conclusion Intracoronary infusion of non-expanded PBMNCs promotes improvement of LV systolic function. This less invasive and more feasible approach to collecting endothelial progenitor cells may provide a novel therapeutic option for improving cardiac function after AMI. (*Circ J* 2007; **71:** 1199–1207)

Key Words: Acute myocardial infarction; Angiogenesis; Cardiac function; Peripheral blood-derived mononuclear cells

Differentiation of mesodermal cells to angioblasts and subsequent endothelial differentiation was believed to exclusively occur in embryonic development[1] but this dogma was overturned when human adult peripheral blood mononuclear cells (PBMNCs) were demonstrated to differentiate into the endothelial lineage[2] These cells named "endothelial progenitor cells" (EPCs) expressed endothelial markers, and were incorporated into the sites of ischemia[3,4] We have recently demonstrated that bone marrow mononuclear cells (BMMNCs) contain EPCs in the $CD34^+$ cell fraction and various proangiogenic factors, such as basic fibroblast growth factor (bFGF), vascular endothelial growth factor (VEGF), and angiopoietin 1 in the $CD34^-$ cell fraction, and that implantation of BMMNCs into the site of ischemia enhances angiogenesis via harmonic supply of EPCs and angiogenic factors[5,6] This technique has been used clinically and developed as a useful therapeutic option for human critical limb ischemia[7]

The concept of the heart as an organ composed of terminally differentiated myocytes incapable of regeneration is also being challenged[8–10] Although attempts to replace necrotic tissue by transplanting other cells (eg, fetal cardiac myocytes or skeletal myoblasts) succeeded in reconstituting heart muscle, these cells failed to completely integrate structurally and to display characteristic physiological function[11–13] In contrast, bone marrow cells (BMCs) have the ability to differentiate into various tissue and are likely to

(Received January 17, 2007; revised manuscript received March 28, 2007; accepted April 24, 2007)

*Departments of Cardiovascular Medicine, *Blood Transfusion and Cell Therapy, **Radiology, †Hematology and Oncology, Kyoto Prefectural University School of Medicine, ††Department of Transfusion Medicine and Cell Therapy, Kyoto University Hospital, Kyoto and ‡First Department of Medicine, Nara Medical University, Kashihara, Japan*

Mailing address: Tetsuya Tatsumi, MD, Department of Cardiovascular Medicine, Kyoto Prefectural University School of Medicine, Kawaramachi-Hirokoji, Kamigyo-ku, Kyoto 602-8566, Japan. E-mail: tatsumi@koto.kpu-m.ac.jp

regenerate myocardium by inducing myogenesis and angiogenesis, as shown by improved cardiac function and myocardial perfusion in recent accumulating evidence from animals and humans[14–17] In particular, cardiac transfer of BMC-derived stem/progenitor cells can have a favorable impact in patients with acute myocardial infarction (AMI).[18,19] Clinical efficacy of intracoronary transplantation of BMCs after AMI has been the focus of recent large scale, randomized, and controlled trials. The potential benefit of intracoronary injection of BMCs for left ventricular (LV) function was reported in the randomized Bone marrow transfer to enhance ST-elevation infarct regeneration (BOOST) trial[20] and in the Reinfusion of Enriched Progenitor Cells and Infarct Remodeling in Acute Myocardial Infarction (REPAIR-AMI) trial.[21] In contrast, intracoronary injection of BMCs after AMI did not significantly improve LV function in the Autologous Stem-Cell Transplantation in Acute Myocardial Infarction (ASTAMI) trial[22] or in the trial reported by Janssens et al.[23] Thus, the latest randomized clinical studies for transplantation of BMCs against AMI retain discrepancies that must be resolved in future trials.

We have previously reported that NOGA-catheter based implantation of non-expanded PBMNCs alone can significantly improve systolic function in ischemic hibernating myocardium of pigs,[24] and that intramuscular injection of human PBMNCs markedly increases regional blood flow in hindlimb ischemia by releasing potent angiogenic factors such as VEGF and bFGF.[25] Moreover, it has been demonstrated that EPCs are indeed mobilized in patients with AMI, peak at 7 days after the onset,[26] and that stromal-cell-derived factor-1 (SDF-1), an important stem cell homing factor, is expressed in the myocardium immediately after AMI.[27] Because the invasiveness of BMC collection in the acute phase of AMI limits its clinical application, we hypothesized that transplantation of non-expanded PBMNCs would even improve the cardiac function in patients with AMI. In this context, we started a clinical trial named the "Japan Trial for Therapeutic Angiogenesis by Cell Transplantation of Peripheral Blood-derived Mononuclear Cells for Acute Myocadial Infarction (TACT-PB-AMI)" in 2004. The primary aim of our study was to examine whether intracoronary injection of non-expanded PBMNCs results in an improvement in LV function, as measured by LV ejection fraction (LVEF), after AMI. Additional objectives were to test the feasibility and safety of this treatment, as well as to assess the effectiveness on regional wall motion, cardiac volumes, and arrhythmias.

Methods

Patients and Study Protocol

Patients between 18 and 80 years of age were eligible for inclusion in the study if they had a first acute ST-elevation myocardial infarction with occlusion of the proximal left anterior descending (LAD) coronary artery and a creatine kinase (CK) level >1,000 IU, which was successfully treated by percutaneous coronary intervention (PCI) within 24 h. According to previous observations,[28,29] CK values were serially measured every 4 h for 24 h after the onset of AMI. Exclusion criteria were the presence of cardiogenic shock requiring intravenous pressors or intra-aortic balloon counterpulsation, pulmonary edema, advanced hepatic or renal dysfunction, evidence of malignant diseases, or unwillingness to participate. Because the patients were best suited for an evaluation of LV function by angiographic imaging, we decided to include only patients with anterior wall infarction. This study protocol was approved by the Ethics Review Board of Kyoto Prefectural University School of Medicine, and written informed consent was given by each patient.

The study was designed as an open-label and non-randomized clinical trial. Briefly, after successful PCI (TIMI III), patients were assigned to either the control (PCI alone) group or non-expanded PBMNC group that received intracoronary infusion of PBMNCs within 5 days after PCI. Intracoronary cell transplantation was performed by over-the-wire balloon catheter. Neither collection of PBMNCs nor sham injection was performed in the control group. The primary endpoint was the global LVEF change from baseline to 6 months' follow-up.

Catheterization Procedure for Progenitor Cell Transplantation

A mean of 2.5±0.5 days after the AMI, an over-the wire balloon catheter was advanced into the infarct-related artery (eg, LAD). To allow for adhesion and transmigration of the infused cells through the endothelium, the balloon was inflated inside the stent previously implanted during the acute reperfusion procedure with low pressure to block blood flow for 3 min while 3.3 ml of the PBMNCs suspension was infused distally to the occluding balloon through the central port of the balloon catheter, as previously described.[19] This maneuver was repeated 3 times to accommodate infusion of the total 10-ml cell suspension, interrupted by 3 min of reflow by deflating the balloon to minimize extensive ischemia. After completion of intracoronary cell transplantation, coronary angiography was repeated to ascertain vessel patency and unimpeded flow of contrast material.

Preparation of Progenitor Cells

A cell separator apheresis system with computer software (COBE Spectra, software version 6.1, Gambro BCT, Lakewood, Co, USA) was used to collect all PBMNC products via the standard MNC program. Acid citrate dextrose-A (ACD-A, Baxter Healthcare Corporation, Deerfield, IL, USA) was used as the anticoagulant at a whole body-to-ACD ratio of 20–25:1 in combination with 2,000 IU heparin sulfate. Apheresis was performed through central venous access from the femoral vein in all patients in the PBMNC group. With the aim of processing the largest amount of blood in the shortest possible time, apheresis procedures were performed with the highest possible but still tolerable blood flow rate, such as 55 ml/min. No more than 2.5-fold of the donor's blood volume was processed on a single day. We usually obtain PBMNCs ($\approx 5\times10^9$ cells) from patients by COBE spectra-apheresis and concentrate them to 10 ml by density gradient centrifugation (Kubota 9810, Japan).

After PBMNCs were harvested by COBE Spectra, 100 μl of the cell suspension was diluted by PBS(–) containing 0.5% bovine serum albumin (Fraction V, Sigma, St Louis, MO, USA) used for flow cytometric analysis. The cells were stained with allophycocyanin-conjugated (APC)-anti-human CD34 (Becton Dickinson, San Jose, CA, USA) and phycoerythrin-conjugated (PE)-anti-human VEGFR2 (KDR) (R&D Systems, Minneapolis, MN, USA).

Appropriate isotype controls were used for each staining procedure; 1×10^5 cells were gated within the lymphocyte region on forward-scatter vs side-scatter plots using a FACS Calibur (BD Bioscience). Next, the percentages of cells in

Table 1 Clinical Characteristics of the Study Population

	Control group (n=36)	PBMNC group (n=18)	p value
Age, years	60.4±11.3	61.8±8.7	0.65
Male sex, no. (%)	32 (88.9)	15 (83.3)	0.57
Hypertension, no. (%)	16 (44.4)	11 (61.1)	0.25
Hyperlipidemia, no. (%)	20 (55.6)	12 (66.7)	0.43
Diabetes, no. (%)	12 (33.3)	5 (27.8)	0.68
Smoking, no. (%)	20 (55.6)	12 (66.7)	0.43
PAD, no. (%)	3 (8.3)	1 (5.6)	0.71
Killip class on admission	1.20±0.48	1.22±0.43	0.66
Infarct segment	6.3±0.5	6.6±0.5	0.06
Vessel diameter, mm	3.24±0.38	3.22±0.31	0.89
Peak creatine kinase, IU/dl	3,764±2,506	4,255±1,615	0.47
Time to revascularization, h	6.1±5.7	5.2±2.4	0.49
Mean transplanted cells, no.	–	$4.92\pm2.82\times10^9$	
Medication			
ACEI, no. (%)	26 (72.2)	15 (83.3)	0.37
ARB, no. (%)	11 (30.6)	5 (27.8)	0.83
β-blocker, no. (%)	19 (52.8)	10 (55.6)	0.85
Diuretics, no. (%)	6 (16.7)	3 (16.7)	1.00
Statins, no. (%)	22 (61.1)	11 (61.1)	1.00

Values are expressed as mean±SD.
PBMNC, peripheral blood mononuclear cell; PAD, peripheral arterial disease; ACEI, angiotensin-converting enzyme inhibitor; ARB, angiotensin-receptor blocker.

each population described below were calculated using CELLQuest software (BD Bioscience).

LV Angiography

LV angiograms were obtained according to standard acquisition guidelines immediately after PCI and at 6 months' follow-up. LVEF and LV volumes were calculated by the area–length method, and regional wall motion was determined with the use of the centerline chord method.

Measurement of Other Parameters

For the assessment of regional LV wall motion, echocardiography was carried out before cell transplantation and at 6 months' follow-up. Two-dimensional resting echocardiography was performed in the 4 standard views (parasternal long-axis and short-axis views and apical 4- and 2-chamber views) and regional LV wall motion analysis was performed as described by the Committee on the Standards of the American Society of Echocardiography, dividing the left ventricle into 16 segments and scoring wall motion as 1=normal, 2=hypokinesis, 3=akinesis, 4=dyskinesis for each segment. The wall motion score index (WMSI) was calculated as the sum of the scores of the segments divided by the number of the segments evaluated at the day of cell transplantation and 6 months' follow-up.

We performed resting Tc-99m (^{99m}Tc)-tetrofosmin gated single photon emission computed tomography (SPECT) before hospital discharge and at 6 months' follow-up. In all patients, 592 MBq of ^{99m}Tc-tetrofosmin was intravenously injected at rest. Immediately after the injection, each patient drank a glass of milk to accelerate tracer clearance from the hepatobiliary system. Data acquisition for SPECT imaging was performed at 30 min after ^{99m}Tc-tetrofosmin injection, using a rotating digital gamma camera (Picker PRISM IRIX) equipped with a low energy, high resolution, and parallel-hole collimator. Reconstructed transaxial images were reoriented in the vertical long-axis and short-axis of the LV. The basal and midventricular segments on short-axis views of the LV myocardium were divided into 8 segments each, and 16 segments were taken. An apical region on the vertical long axis was also taken, and a total of 17 segments were analyzed. The ^{99m}Tc-tetrofosmin perfusion defects were visually evaluated by 2 experienced observers, who had no knowledge of the patient's clinical information, with a 5-point grading system (0=normal, 1=mildly decreased uptake, 2=moderately decreased uptake, 3=severely decreased uptake, 4=defect). The grading was decided on by consensus between the 2 observers, and the sum of the scores for all segments was used as the defect score.

To assess whether intracoronary cell transplantation was associated with proarrhythmic effects, we performed 24-h Holter recording for all patients before hospital discharge and at 6 months' follow-up, and estimated the Holter Lawn class by calculating premature ventricular complexes and ventricular tachycardias.

Follow-up Examinations

Six months after progenitor cell therapy, cardiac catheterization was repeated; left ventriculography was performed with identical projections and adequate contrast opacification for quantitative analysis according to standard guidelines and coronary angiograms were analyzed for the presence of restenosis in the infarct-related artery. Echocardiography, Holter ECG, and perfusion scintigraphy were also repeated after 6 months.

Statistical Analysis

Continuous variables are presented as means±SD. Control and cell therapy groups were compared using the chi-square test for discrete variables and unpaired Student's t-test for continuous variables according to standard statistical methods. Statistical significance was assumed at a value of $p<0.05$. All statistical analysis was performed with SPSS (Version 9.0, SPSS Inc, Chicago, IL, USA).

Results

Baseline Characteristics and Procedural Results of Cell Infusion

The clinical characteristics of the study population are